JAERI-M
6549

MEASUREMENT OF MULTIPLE CONTROL RODS REACTIVITY WORTHS IN SEMI-HOMOGENEOUS CRITICAL ASSEMBLY

May 1976

Y. KANEKO, F. AKINO, H. YASUDA, R. KUROKAWA,
K. KITADATE and M. TAKEUCHI

日本原子力研究所
Japan Atomic Energy Research Institute

この報告書は，日本原子力研究所が JAERI-M レポートとして，不定期に刊行している研究報告書です．入手，複製などのお問合わせは，日本原子力研究所技術情報部（茨城県那珂郡東海村）あて，お申しこしください．

JAERI-M reports, issued irregularly, describe the results of research works carried out in JAERI. Inquiries about the availability of reports and their reproduction should be addressed to Division of Technical Information, Japan Atomic Energy Research Institute, Tokai-mura, Naka-gun, Ibaraki-ken, Japan.

JAERI-M 6549

Measurement of Multiple Control Rods Reactivity Worths in Semi-Homogeneous Critical Assembly

Yoshihiko KANEKO, Fujiyoshi AKINO, Hideshi YASUDA,
Ryosuke KUROKAWA, Kenji KITADATE and Motoyoshi TAKEUCHI

Division of Reactor Engineering, Tokai JAERI

(Received April 26, 1976)

Experimental and theoretical works are described which have been made to obtain the experimental techniques of determining large negative reactivity worths as accurately as practicable.

Measurements are first made on reactivity effect of the experimental multiple control rods arranged in ring by the pulsed neutron method in the Semi-Homogeneous Critical Assembly, a heavily reflected graphite-moderated 20 % enriched multiplying system. The atomic ratios of C to ^{235}U in the core region are 2226 and 6628 in the SHE-8 and SHE-T-1 cores respectively. Subcriticality is determined in the static reactivity from the measured prompt neutron decay constants by making resonable, large correction to the well-known King-Simmons formula due to change of the neutron generation time estimated by calculation. Measured reactivity worths of the multiple control rods thus obtained are in good agreement with those by two-group diffusion calculation.

New multi-point type formulas are then given which replace the single-point type expressions for methods of "area-type" pulsed-neutron, source multiplication, and rod drop. In the formulas, the reactivity value is derived by integrating all the neutron counting data from every part of the reactor core to sweep out effects of the kinetic distortion and the spatial harmonics. Experiments made for SHE-T-1 are to examine the proposed integral versions and to confirm validity of the King-Simmons formula with large correction for the change of neutron generation time. The numbers of measuring points in each core are 16 and 48 for the pulsed neutron and the rod drop method, and for the source multiplication method, respectively. Space dependence of the experimental results obtained by the single-point type formulas is up to $\sim$ 40 % for each of the experimental methods. To reduce the larged machine time, a four-channel counting device is used.

The polarity correlation method finally is applied to the experiment to measure the reactivities from critical to nearly shut-down state (-12 $) in both SHE-8 and SHE-T-1 which have large neutron lifetime of $\sim$ 1 ms. The measured results are in fairly good agreement with those by the pulsed neutron method using the King-Simmons formula and by the rod drop method.

JAERI－M 6549

半均質臨界実験装置における多数本制御棒の反応度価値測定

日本原子力研究所東海研究所原子炉工学部
金子義彦・秋濃藤義・安田秀志・黒川良右
北館憲二・竹内素充

（１９７６年４月２６日受理）

多数本の制御棒価値をはじめ，大きな負の反応度測定技術の研究開発について，半均質臨界実験装置において行われた活動をまとめたものである。まず，第一に増倍系における離散的固有値の存在に関する理論的，実験的考察を行うと共に，その測定においては，遅発中性子モードの減衰を考慮したunfolding法の適用が必要であることを指摘した。つぎに，SHE－8及びSHE－T１炉心における多数本制御棒の反応度価値の測定に対する改良形King－Simmons法のパルス中性子法の適用についてのべた。さらに，同じ実験配置について，空間高調波や動的歪曲を包合するために空間積分法による多点観測の有効さを，面積形のパルス中性子法，中性子源増倍法，およびロッドドロップ法について実証して約３５$までの反応度測定が可能であることを示した。最後に極性相関実験法の改良についてのべ～１２$まで測定可能な反応度領域を広げることに成功したことをつけ加えた。

Contents

1. Introduction ---------- 1

2. Basic problems related to the pulsed neutron method-- 3

3. Measurement of reactivity worths of control rods by use of the pulsed neutron method ----------12

4. Integral-versions of area-type pulsed neutron, source multiplication, and rod drop method ----------18

5. Polarity correlation experiment ---------- 25

6. Conclusion ---------- 32

Acknowledgement ---------- 33

References ---------- 34

Tables

Table 1 Physical and nuclear properties of SHE cores

Table 2 Prompt neutron decay constant determined with and without consideration for the slow decay of the delayed-neutron modes

Table 3 Experimental results for reactivity worths of experimental control rods in Ring Geometry in SHE-8 and SHE-T1.

Table 4 Experimental results for the subcriticalities of various core configurations with multiple experimental rods

Figures

Fig. 1 Relaxation time constant of the inverse silver ratios in the graphite pile and the subcritical SHE-6 and -9

Fig. 2 Delayed-neutron effect on determination of prompt neutron decay constant, in a pulsed neutron experiment. Numbers appearing near the calculated points are the period, in second, of neutron pulses.

Fig. 3 Dependence of the value of α resulted by least squares fitting on the initial fitting start time from the pulsed neutron bursts.

Fig. 4 Fuel loading patterns of SHE, and patterns of the experimental control rods configuration

Fig. 5 Block diagram of the measuring system

Fig. 6 Reactivity worths of the experimental control rods in ring geometries

Fig. 7 Correction to the King-Simmons formula due to the change of the neutron generation time

Fig. 8 Mutual interaction among experimental control rods arranged in ring geometry

Fig. 9 Space-dependence of the reactivity values, obtained by single-point type formulas.

Fig. 10 Decay of neutron density following pulsed neutrons stored in 1024 channel time analyzer, 254 channels for each of four neutron counting channels.

Fig. 11 Spatial distribution of the neutron counts in the core region of SHE-T1.

Fig. 12 Decay curves of polarity correlation function against delay time for the various number of safety rods inserted

Fig. 13 Reactivity worths plotted against the number of safety rods inserted

Fig. 14 Conditional polarity correlation function measured at - 20¢ subcritical SHE-VIII-1 against delay time

1. Introduction

This paper summarizes authors' experimental and theoretical works done with purpose to establish the pulsed neutron method, the polarity correlation method and the other experimental methods including the rod drop and source multiplication methods. It is aimed to determine the large negative reactivities of the reactor as accurately as practicable. Experiments were done at Semi-Homogeneous Critical Assembly, SHE, which is a 20 % enriched uranium loaded critical assembly, moderated and reflected with graphite. Many type cores were built at SHE. The atomic ratio of carbon to uranium-235 in the core region was varied to the present from 2228 to 6628. The nuclear and the other physical properties of the cores were listed in Table 1. The most characteristic feature of the cores is that the effect of the graphite reflector, 90 cm thick is very strong on the neutron kinetic behaviours. At first, the problem of neutron thermalization in the multiplying media is discussed in Chap. 2. As also given in this chapter, an improved data unfolding technique for the pulsed neutron method as accurately as possible is developed to find the prompt neutron decay constant regarding the contributions of the delayed neutron modes to the decay of the neutron flux at near critical states. It is because the neutron generation time is prolonged to $\sim$1 ms due to the reflector effect with making the decay of the prompt neutron mades significantly slower. Second, discussions are made how to overcome the kinetic distortion appearing in the

time-decay of the neutron flux after the pulsed neutrons bursts. The original King-Simmons formula can get valid in a limited range of subcriticality and in a limited core configurations. Then, the corrections to the formula with respect to the change of the neutron generation times were atempted, for finding the reactivity values, as described in Chap. 3. Third, the integral versions of the various experimental methods as well as the area-type pulsed neutron method were introduced as described in Chap. 4. In this chapter, inter-comparison among these experimental methods was made as for the negative reactivities down to about 50$, which were realized with insertions of the experimental control rods into the core of SHE-T1. At last, as described in Chap. 5, some improvements are done for the polarity correlation method, with respect to the triggering conditions being limited for the giant families decay as well as the adoption of the large volume neutron detectors, because, due to the prolonged neutron generation time, the correlation amplitudes becomes small.

2. Basic problems related to the pulsed neutron method

Two basic problems related to the pulsed neutron method, which were discussed by the authors, are summarized in this Chapter. One is the neutron thermalization problem in the multiplying media. The other is the data unfolding technique to find the prompt neutron decay constant as accurately as possible from the decay data of the neutron flux observed in the reactor at near critical, sweeping out the contributions of the delayed neutron modes.

2.1 Time-dependent neutron thermalization in multiplying system

The pulsed neutron technique is based on the assumption that there exists a discrete fundamental eigenvalue for the multiplying system under study and that this eigenvalue, that is, the prompt neutron decay constant α, can be measured by observing the decay of neutron flux after pulsed neutron injection. This assumption has not yet been definitely proved valid[1),(2)]. It is generally known that the prompt neutron decay constant α can be given as a fundamental eigenvalue of the characteristic equation, describing the time-dependent neutron thermalization in a multiplying system.

An attempt was made to analyze this problem on the discrete eigenvalue model.[3)]

The analysis was made under the following simplifying conditions:

(1) The system is infinite and homogeneous.

(2) The absorption and fission cross sections $\Sigma_a(E)$ and $\Sigma_f(E)$ are of 1/v type.

The characteristic equation for the multiplying system is given by

$$\begin{aligned}(\lambda_m - \Sigma_{a0} v_0) N_m(E) = {} & v_0 \Sigma_s(E) E^{1/2} N_m(E) \\ & - v_0 \int_0^\infty \Sigma_s(E' \to E) E'^{1/2} N_m(E')\, dE' \\ & - \nu \Sigma_{f0} v_0 \chi(E) \int_0^\infty N_m(E')\, dE'\end{aligned} \tag{1}$$

with neglection of the delayed neutrons, where E is the energy in kT units, v_0 the neutron velocity corresponding to $E_0 = kT$, $N_m(E)$ and λ_m the eigen function and the eigenvalue of the m-th mode, Σ_{a0} and Σ_{f0} the macroscopic absorption and fission cross sections for $v = v_0$ and $\chi(E)$ the energy distribution of the fission neutrons.

Consider a pure non-multiplying system whose neutronic properties are the same as those of the above-mentioned multiplying system except the condition $\Sigma_a(E) = 0$, $\Sigma_f(E) = 0$.

The characteristic equation for this non-multiplying system is

$$\begin{aligned}\lambda'_m N'_m(E) = {} & v_0 \Sigma_s(E) E^{1/2} N'_m(E) \\ & - v_0 \int_0^\infty \Sigma_s(E' \to E) E'^{1/2} N'_m(E')\, dE'.\end{aligned} \tag{2}$$

where $N'_m(E)$ and λ'_m represent the eigen function and the eigenvalue of the m-th mode.

By assuming that $N_m(E)$ can be expanded in terms of $N'_m(E)$, $N_m(E)$ can be given by

$$N_m(E) = \sum_{i=0}^{\infty} A_{mi} N_i'(E) \tag{3}$$

By substituting Eq. (3) into Eq. (1) and making use of the well-known relation[4]

$$\int_0^{\infty} N_i'(E)\, dE = 0 \tag{4}$$

as well as the orthonormal conditions between $N'_i(E)$ and the adjoint function $N'_j(E)$

$$\int_0^{\infty} N_i'(E) N_j'^{*}(E)\, dE = 0, \qquad i \neq j \tag{5}$$

$$\int_0^{\infty} N_i'(E) N_j'^{*}(E)\, dE = 1, \qquad i = j \tag{6}$$

, one can conclude that

$$\begin{aligned} \lambda_0 &= \lambda_0' + \Sigma_{a0} V_0 - \nu_p \Sigma_{f0} V_0 \\ \lambda_1 &= \lambda_1' + \Sigma_{a0} V_0 \\ \lambda_2 &= \lambda_2' + \Sigma_{a0} V_0 \\ &\cdots\cdots \end{aligned} \tag{7}$$

A linear algebra determines the coefficients A_{mj}:

$$\frac{A_{0j}}{A_{00}} = \frac{\nu_p \Sigma_{f0} V_0 \int_0^{\infty} \chi(E) N_j'^{*}(E)\, dE}{\nu_p \Sigma_{f0} V_0 + \lambda_j' - \lambda_0'} \tag{8}$$

$$A_{mj} = 0, \quad for \quad m > 0 \quad m \neq j \tag{9}$$

The above analysis results in the following conclusions,

(1) Introduction of fissionable materials causea a change of the fundamental eigenvalue and of the eigen function as indicated by Eqs. (7) and (8), and reduces all the higher eigenvalues by $\Sigma_{a0}V_0$, but does not at all influence the higher eigen functions.

(2) The thermalization time constant is smaller in the multiplying system, τ_{th}(multi), than in the pure non-multiplying system, τ_{th} (non-multi) of λ'^{-1}_1 because from Eq. (10),

$$\tau_{th}(multi.) = (\lambda_1 - \lambda_0)^{-1}$$
$$= (\lambda_1' - \Sigma_{a0}V_0 + \nu\Sigma_{f0})^{-1} \tag{10}$$

and thus,

$$\tau_{th}(\text{multi}) < \tau_{th}(\text{non-multi}). \tag{11}$$

It must be noted that the above conclusions have been obtained on the discrete eigenvalue model under the simplified conditions described in the beginning of this paper. Theoretical studies on actual non-multiplying systems have previously established that discrete eigenvalues should be limited below $(\nu\Sigma)_{min}$, beyond which there exists a wide region of continuous eigenvalues. This points towards the necessity of further rigorous treatment of this problem in the future.

In order to substantiate the theoretical conclusion expressed by Eq. (11), preliminary experiments were carried out.

The thermalization time constants, τ_{th}(non-multi) for one non-multiplying (a pure graphite system), and τ_{th}(multi) for two multiplying systems (graphite moderated 20 % enriched uranium system) -SHE-6 and 9-were measured by silved filter transmission method. These experimental systems are described in Table 1. Bursts of D-T neutrons with a pulse width of 50 μs were injected approximately into the center of the system under study by using a 150 kV Cockcroft Walton accelerator. Thermalizing neutrons were detected with small BF_3 counters (Twenty-century 40 mmHg)-first bare, and then silver filter covered-placed either in the center of the fuel region or of the graphite pile. The relaxation constant of the counting ratio between the two counters gives the thermalization time constant, and are seen to be strongly dependent on the point in time at which the data fitting is started, but appear to tend toward asymptotic values, which should be the true values of the thermalization time constant τ_{th}. It can be concluded from Fig. 1 that the thermalization time constants τ_{th}(multi) in the multiplying systems in question, namely SHE-VI and -IX, are smaller than the τ_{th}(non-multi) in the non-multiplying system, in the case a graphite pile. Then, it may be safe to say that the existense of the discrete fundamental prompt neutron decay constant is clear in the usual subcritical reactor.

2.2 Effect of Delayed-Neutron Mode on the Determination of the Prompt-Neutron Decay Constant in Pulsed Neutron Measurements[7]

The pulsed-neutron technique has been widely used to measure the prompt-neutron decay constant α of reactors. So far the value of α has usually been determined by fitting the change of the measured neutron count rate, following the source burst, to a single exponential function accompanied by a constant background. This is the constant background method.

It has been pointed out by Küchle[5] and Sastre and Weinstock[6] for near-critical heavy water or graphite-moderated reactors that the use of such a formula will introduce appreciable systematic errors because of the over simplified treatment of the background neutron counts as being constant with time. The background, in fact, should change due to the slow decay of the delayed-neutron modes. The purpose of the present work is to show an improved method of correcting the effect of the gradual buildup of delayed neutrons on the prompt-neutron decay and to evaluate systematically and quantitatively the dependence of the effect on the length of neutron lifetimes, on the subcriticality of a reactor, and also on the repetition rate of neutron pulses. The method presented below is an improvement over those described in Refs. 5 and 6 in the following two respects. One is the consideration of the post-burst neutrons. Another is the adoption of a simpler estimate of the relative amplitude of the prompt-neutron mode. The principle of the method is described in Ref. 7. A computer code[8] ALPHA-D has been developed to treat the experimental data for near-critical reactors.

The validity of the present method is established by the comparison of the results of its application to the following

test problems or the example experimental data with those obtained by earlier methods.

Ten sets of test problem are provided in the form of the counts per channel by calculations using the numerical time-step methods for representative subcritical reactors from criticality down to about one dollar subcritical, having a neutron lifetime of 1 msec or 100 μsec. The period of the neutron pulses is changed to 5, 2, and 1 sec. Three different methods were applied to the problems. The first and second are the present method and the constant-background method, respectively. The third is essentially the same as the earlier method of Refs. 4 and 5 from the viewpoint of neglecting post-neutron pulses. The results of the applications of the three different methods to the test problems are shown in Fig. 2. It is clear from the figure that the present method yields correct values of the prompt-neutron decay constants of slightly subcritical reactors having a 1-msec neutron lifetime which are free from systematic errors of $\sim$ 5% which would be inevitable with the constant background method. It is further shown that its use is effective not only for a slightly subcritical reactor (0 to 10 cents) but also for reactors as much as two dollars subcritical because the systematic error amounts to $\sim$ 2% in the constant background method. The systematic errors introduced in the constant back-ground method become larger as the period of the neutron pulses becomes shorter. For the shortest period, 1 sec, the error should amount to -4.9 % for the reactor with a decay constant of 8 sec^{-1}.

The effect of the post-pulse neutrons on the determination of decay constants is checked by the comparisons of the results of the present method with those of the third method; the results of the third method are smaller than the correct value of 8 sec^{-1} by 0.1, 0.2, 0.5, and 1.1 % for the repetition periods of 10, 5, 2, and 1 sec, respectively.

It is also found that the experimental data for the reactors having the short-neutron lifetime of 100 μsec can be treated within the systematic error of 1% with the constant background method.

Experimental data for SHE-5 at near criticality were processed by both the present and the constant background methods. This assembly has a neutron lifetime of 1.18 msec,[9] measured by a pulsed-neutron technique, due to the strong reflector effect. It was operated at 51.75 and 66.9 cents subcritical. The resulting values of α determined by the two methods differed by $\sim$ 4 % (Table 2). The dependence of the value of α resulted from the two different computor codes ALPHA-D and ALPHA (constant background method) on the initial fitting start time is illustrated in Fig. 3 as for the SHE-T-1 core at 18.5 ¢ subcritical, saturation tendency of α with the initial fitting start time can not be observed with the latter computor code. Both results are consistent with the tendencies experienced in the test problems.

It is clear from the arguments given above that the present method is improved over earlier ones in the following ways:

1. The first and second post-neutron pulses are considered

for the estimation of the amplitudes of the dealyed neutron modes which were disregarded in earlier work. The consideration is unnecessary in the case of the long repetition period, T = 10 sec, but is necessary in the case of shorter repetition periods, 1 sec. Use of such short periods is essential when the time allowed for the measurement is restricted as, for example, in the reactivity measurement for reactor startup.

2. The amplitudes of the delayed-neutron modes can be estimated in each iteration from the value of the prompt-neutron decay constant α determined by least-squares fitting of the neutron counts in the time after higher spatial harmonics have died away.

It is concluded that the application of the present method to the determination of α from the measured neutron counts removes the systematic error due to the delayed-neutron modes. It is applicable to heavy water or graphite moderated reactors, having neutron lifetimes of the order of 1 msec, ranging from critical reactors to a few dollars subcritical. The method is especially applicable when the the period of the neutron pulses is short. Even for light-water-moderated reactors, the use of the present method is preferable to remove a small systematic error of the order of 1%.

3. Measurement of reactivity worths of control rods by use of the pulsed neutron method

Measurements on the reactivity effect of the experimental multiple control rods, arranged in ring geometry were undertaken with the application of the pulsed neutron method using the King-Simmons formula in SHE-8 and SHE-T-1 core. Both of the two cores are side-reflected cylindrical ones, whose atomic ratio of C to ^{235}U is 2226 and 6629 respectively [9]. The latter core is slightly loaded also with thorium oxide fuels. The nuclear properties of the two cores are summarized in Table 1, and the fuel loading patterns are shown in Fig. 4.

The experimental control rods are provided by inserting the hollow neutron absorbing pellets into the thin aluminum tubes. The pellets which are the cold-pressed mixture of the natural graphite and B_4C powders with the average boron content of 10 w/o and with gross density of 2.02 g/cm^3, and are 50 and 30 cm in outer and inner diameter, respectively. The number of the experimental control rods, fully inserted at the same time, is varied from one to six. The patterns of the experimental control rods configurations are of ring geometry as illustrated in also Fig. 4 in case of three experimental control rods.

The pulsed neutron source used (JAERI-ToshibaNP-11-PT) was a 200 KV Cockcroft type neutron generator[10]. In this generator, the pulsed ion beam is obtained by modulating both the extraction voltage at the probe of the ion source and the

deflecting voltage for the accelerated ion beam. On extension tube with a T target is placed horizontally in the hollow graphite tube (MC 9 in Fig. 3). The ratio of the peak neutron output to the background is over 10^5. About 10^6 neutrons/burst are obtained with 100 μsec pulse width. The repetition frequencies range from 0.1 to 10 p.p.s., depending on the value of the subcriticality.

A block diagram of the measuring system is shown in Fig. 5. A BF_3 counter (Hitachi EB 125.5) 2.5 cm diameter is inserted into the hollow graphite tube MB4 at a distance of 30 cm from the mid plane (See Fig. 4). The position of the detector is determined to satisfy the requirement that the component of the several spatially higher harmonics can be eliminated in the detection of neutrons. The neutron-induced pulses from the counter are amplified and discriminated from noise, and then fed to the 256 channel TMC time analyzer making use of the pulsed neutron unit 212.

The prompt neutron decay constants of the fundamental mode α are determined from the decay data of the neutron density stored in the time analyzer. The raw data were fitted by least squares method to a single exponential type formula after correction for counting loss using a computer code ALPHA[11] for most cases and ALPHA-D[8] for the particular cases at near critical, as described in Chap. 2. The most probable value of α determined through the above procedure is further affected by the time initial point of the fitting, due to the appreciable contribution provided by spatial harmonics to the prompt

neutron decay. However, even in the worst case, the value of α saturated after an elapse of ~ 20 msec. The measured values of the prompt neutron decay constants, thus determined are listed in Table 3. The experimental errors including statistical and systematic one are mostly estimated within 1 %.

The change of the prompt neutron decay constant by inserting the experimental control rods into the slightly subcritical cores being called as the standard state hereafter is very valuable, because adopting this change as the measure of the subcriticality the direct comparison between experiment and theory can be possible, but such is significantly not easy problem with respect to the static reactivity.[12]

The worths for each of the experimental control rods configuration are determined as shown in Fig. 6 in scale of the static reactivity ρ from the measured prompt neutron decay constants α making the reasonable but very large correction to the well-known King-Simmons formula due to the change of the neutron generation estimated by calculation. The correction is made by the following procedure.

The King-Simmons formula is

$$\frac{\rho_{KS}}{\beta_{eff}} = \frac{\alpha - \alpha_c}{\alpha_c} \qquad (12)$$

where α_c stands for the prompt neutron decay constant at critical state.

Considering the change of the neutron generation time ℓ_f the King-Simmons formula is corrected as[13]

$$\frac{\rho_{RKS}}{\beta_{eff}} = \frac{\alpha - \alpha_c}{\alpha_c} \cdot f + \varepsilon_1 + \varepsilon_2 \tag{13}$$

$$f = \frac{1}{\beta_{eff}} \sum_i \frac{\alpha_c \beta_{i\,eff}}{\alpha_c - \lambda_i} \tag{14}$$

$$\varepsilon_1 = \left(\frac{l_j}{\beta_{eff}} - \frac{l_{gc}}{\beta_{eff\,c}} \right) \cdot \alpha \tag{15}$$

$$\varepsilon_2 = \frac{1}{\beta_{eff}} \sum_i \frac{\alpha \beta_{i\,eff}}{\lambda_i - \alpha} - \frac{1}{\beta_{eff\,c}} \sum_i \frac{\alpha_c \beta_{i\,eff\,c}}{\lambda_i - \alpha_c} \tag{16}$$

In from Eqs. (12) to (16), the commonly used notations are utilized, with subscript c refering to the critical state. The correction factor f shows small deviation of α_c from β_{eff}/l_{gc} in the order of 9 %, and never be less important. The correction expressin in ε_1 due to the change of l_g followed by the insertion of the experimental control rods is most important. The another correction expressed in ε_2 is so small as negligible in most cases.

The change of l_g is estimated by calculating both of α and ρ for each subcritical states and substituting both results into the equation

$$l_j = \frac{-\rho}{\alpha} + \sum_i \frac{\alpha \beta_{i\,eff}}{\lambda_i - \alpha} \tag{17}$$

This calculations was made using a computer code CRODER, which solves the two-dimensional diffusion equation by the source

sink method. The calculated correction terms of f, ε_1 and ε_2 are also listed in Table 3 and the space-dependence of ε_1 is shown in Fig. 7. It is to be noted here that this correction terms amount up to $\sim$ 100 % of the reactivity values evaluated by the original King-Simmons formula, when the experimental control rods are gathered in the central part of the cores, the reactivity being down to about $\sim$ 50 \$. This situation is due to the fact that the neutron populations are let to be higher in the peripherical regions of the core-reflector boundaries.

In order to summarize the experimental results, it is logical to define the interference factor S as a measure of the mutual interaction among the multiple control rods by the equation.

$$S = \frac{\rho_N}{N \rho_1} \tag{18}$$

where ρ_1: reactivity worth of a single control rod

ρ_N: reactivity worth of a ring of N control rods

The factor S exceeds unity in the case of antishadowing, and is smaller than 1 in the case of shadowing. The dependences of S on the distance between the most adjacent two control rods are shown in Fig. 8.

It is to be noted from observation of Fig. 8 that the reactivity worths of the multiple control rods arranged in a ring geometry show good agreement between experiment and calculation. It may be essentially because in calculation the extrapolation distance for the fast group neutrons at the

surface of the experimental control rods was so adjusted as to equalize the calculated value of the fully inserted single central rod with the measured value: Measured value of $\alpha - \alpha_c$ = calculated value of $\alpha - \alpha_c$.

4. Integral-Versions of Area-Type Pulsed Neutron, Source Multiplication, and Rod Drop Method

Theoretical treatments, including the methods of source-multiplication, rod-drop and source-jerk, are suggested in the authors' paper of Ref. 14 for dealing with the spatial effects observed in several kinetic experiments for determining large negetive reactivity in a reactor.(14) An analysis by means of kinetic eigenfunctions is made on the kinetic behavior of the reactor, when these methods are applied. For each kind of experiment, a new multi-point type formula is established to replace the current single point type expressions, in order to derive the precise reactivity value by utilizing all of the neutron counting data obtained from every part of the reactor core. In the new formulas, the raw neutron counting data are integrated in reference to space and energy, weighted with the product of the static adjoint function $n^{+}(\vec{r},v)$ and the static fission spectrum $f_s(v)$. This integral procedure is effective in eliminating the effects of kinetic distortion and of the spatial harmonics included in the raw counting data. The new formulas as well as one for the pulsed neutron method, given by Kosaly et al.(15), are summarized here.

Pulsed neutron method:

$$\frac{\bar{\rho}_{sJ}}{\beta_{eff}} = \frac{\bar{A}_p}{\bar{A}_d} \qquad (19)$$

Source multiplication method:

$$\bar{\rho}_{sM} = \frac{S\, n^{+}_{os}(\vec{r}_s, v_s)}{\bar{A}_t} \qquad (20)$$

Rod-drop method : (Source-jerk)

$$\frac{\bar{\rho}_{ROD}}{\beta_{eff}} = \frac{\bar{A}_c}{\bar{\lambda}\ \bar{A}_r} \tag{21}$$

Remarks:

(1) $$\bar{A}_p = \int_V d\vec{r}\, A_p(\vec{r}) \int_0^\infty n_{os}^+(\vec{r}, v') f_s(v')\, dv' \tag{22}$$

$$\bar{A}_d = \int_V d\vec{r}\, A_d(\vec{r}) \int_0^\infty n_{os}^+(\vec{r}, v') f_s(v')\, dv' \tag{23}$$

(2) d = Proportional constant

(3) $n_{os}^+(\vec{r}_s, v_s)$ = Value of the adjoint function for extraneous source neutrons

$$\bar{A}_t = \int_V d\vec{r}\, A_t(\vec{r}) \int_0^\infty n_{os}^+(\vec{r}, v') f_s(v')\, dv' \tag{24}$$

(4) $$\bar{A}_c = \int_V d\vec{r}\, A_c(\vec{r}) \int_0^\infty n_{os}^+(\vec{r}, v') f_s(v')\, dv' \tag{25}$$

$$\bar{A}_r = \int_V d\vec{r}\, A_r(\vec{r}) \int_0^\infty n_{os}^+(\vec{r}, v') f_s(v')\, dv' \tag{26}$$

$\bar{\lambda}$ = Average decay constant of the delayed neutrons precursors

where $A_p(\vec{r})$ = area of the promp neutron modes

$A_d(\vec{r})$ = area of the delayed neutron modes

$A_t(\vec{r})$ = counting rate of the neutrons multiplicated from the source neutrons

$A_c(\vec{r})$ = counting rate of the neutrons before the rod drop

$A_r(\vec{r})$ = total neutron count after the rod drop

Experiments are undertaken at SHE-T1 core with purpose to examine the integral versions of the experimental methods, proposed above. Certainly it is intended to clarify the measurable range of reactivity worth to be enlarged, the accuracies to be improved, and the machine time to be lengthened. According to such purpose, five core configurations are adopted to be operated with the different experimental methods. As listed in Table 4 and Fig. 9, the core configurations, named as 1C, 2C, and 3C, are made subcritical with full insertions of one, two, and three experimental control rods into the SHE-T1 core at -11.1 ¢ subcritical, respectively, and are the same with some of those adopted in the experiments described in Chap. 3. This is because the validity of the correction procedure is also aimed to be checked. On the other hand, the core configuration named as 6S, which is made subcritical with half insertion of the six control rods equipped to SHE for the usual operation is adopted for comparison between the pulsed neutron method and the rod drop method. The another core configuration named as 0C, which is made subcritical with unloading three fuel rods from the critical core, is adopted, because its subcriticality was safely estimated as -81.3 ¢ from the worths of the fuel rods measured by the period method, then this core configuration being appropriate for use as the standard state for the estimation of the neutron source strength in the source multiplication method. The core configurations, illustrated above, are let to be written simply as 0C, 1C, 2C,

3C, and 6S hereafter. The number of the measuring points for each core configuration is 16 and 20 ~ 48 in case of the pulsed neutron and the rod drop method and in case of the source multiplication method, respectively, and is illustrated in Fig. 9.

The experimental control rods, named as "Gray 50/30", are provided by inserting the neutron absorbing pellets (O.D. 50 mm, I.D. 30 mm) into the thin aluminum hollow tubes. In the source multiplication method, a 100 mCi Am-Be neutron source was positioned at the center of the cores, except C1 core, as shown in Fig. 9. With the view to shorten the machine time, the brock diagram for the measurement shown in Fig. 5 was so improved as illustrated in the same figure. First, four neutron counting channels are provided using small BF_3 counters (Twenty Century 5 EB 60/6) with diameter of 1/4". The reactivity decrease due to the BF_3 counters were as well as 7.3 ¢ at most. Second, a ND-2200 1024 channel analyzer is operated with a home-made controller to analyze the time-dependence of the neutron signals in 256 channels for each of the different four counters.

The values of adjoint functions required as the weight for the space-integration are obtained by two groups diffusion approximation, using the computer code EQ-3.[16]

Reactivity worths by the area-type pulsed neutron method are obtained as follows. The time-distributions of the neutron signals after the neutrons bursts, stored in the time analyzer as shown in Fig. 10, are fitted to the single exponential type

decay using the computer code ALPHA[11]. Then, both the value of α and the constant background level are determined, the integration of the latter between the period of the two succesive pulsed neutrons bursts giving the values of $A_d(\vec{r})$. The values of $A_p(\vec{r})$ are obtained by subtracting $A_d(\vec{r})$ from the total area composing of prompt plus delayed neutron modes which can be simply determined by summing up every neutron counts between the succesive neutrons bursts. Dependence of $A_p(\vec{r})/A_d(\vec{r})$ on the measuring points is slight in OC, but is significant in the other more far subcritical states. This situation is shown in Fig. 9. The reactivity worth determined by integrating those space-dependent areas according to Eq. (19) are listed in Table 4. In the integration procedure, the whole core volume V was divided into the sub-volumes V_i so as each containing one detector position. Then the following approximation is made;

$$\int_{V_i} d\vec{r}\, A_p(\vec{r}) \int_0^\infty n_{os}^+(\vec{r}, v')\, f_s(v')\, dv' \doteq V_i\, n_1^+(\vec{r}_d)\, A_p(\vec{r}_d) \qquad (27)$$

and

$$\int_{V_i} d\vec{r}\, A_d(\vec{r}) \int_0^\infty n_{os}^+(\vec{r}, v')\, f_s(v')\, dv' \doteq V_i\, n_1^+(\vec{r}_d)\, A_d(\vec{r}_d) \qquad (28)$$

where $n_1^+(\vec{r}_d)$ stands for the calculated fast group adjoint function at the detector position $\vec{r}_d$ in the sub-volumes.

The reactivity worth by the source multiplication method are obtained as follows. As for the volume integration of $A_t(\vec{r})$ which was measured as the spatial distribution of the

neutron counting rate as shown in Fig. 11, an approximation is adopted,

$$\int_{V_i} d\vec{r}\, A_1(\vec{r}) \int_0^{\infty} n_{os}^{+}(\vec{r}, v') f_s(v')\, dv' \doteqdot V_i\, w_i\, A_t(\vec{r}_d) \qquad (29)$$

with

$$w_i = \frac{\int_{V_i} d\vec{r}\, n_1^{+}(\vec{r})\, \phi_2(\vec{r})\, d\vec{r}}{V_i\, \phi_2(\vec{r}_d)} \qquad (30)$$

where $n_1^{+}(\vec{r})$ and $\phi_2(\vec{r}_d)$ represent the calculated fast group adjoint function and the thermal neutron flux at position $\vec{r}_d$, respectively.

It is very important to calculate presice value of $n_{os}^{+}(\vec{r}_s, v_s)$: This value was obtained by the four group diffusion theory with making the highest energy group to include the source neutrons from the Am-Be neutron source.

The reactivity worth by the rod drop method is obtained only for 6S. The measured values of $A_c(\vec{r})/A_r(\vec{r})$ showed strong space-dependence as shown in Fig. 9. The reactivity worth obtained by integrating $A_c(\vec{r})$ as well as $A_r(\vec{r})$ according to Eq. (21), is listed in Table 4, where some approximation is used similar to Eqs. (29) and (30).

It can be concluded from observing of the experimental results summarized in Table 4 that agreement of the measured reactivities is markedly improved among the different experimental methods:

(1) Difference between ρ_{RKS} and ρ_{SJ} is within only 5 % down to $\sim$ 48\$ (0C,1C,2C,3C cores)

(2) Difference between $\bar{\rho}_{SJ}$ and $\bar{\rho}_{SM}$ is also not appreciable to $\sim$ 34\$ (0C,1C,2C), although it is very large for the most highly subcritical cores, 3C, whose negative reactivity is $\sim$48\$.

(3) In case of 6S core, $\bar{\rho}_{ROD}$ agreed comparatively well with the other reactivity values of $\bar{\rho}_{SJ}$, ρ_{RKS} and $\bar{\rho}_{SM}$, where all the weights are simply assumed as unity. Three-dimensional diffusion calculation are being done in order to obtain the precise weighting factor expressed by Eq. (30).

5. Polarity correlation experiment

5.1 Introductory to polarity correlation

The reactor noise analysis, including the polarity correlation method, has been used to determine the correlation function of neutron count rate mainly in fast and light-water moderated reactors. It has little been used for graphite or heavy-water moderated reactors with long prompt neutron lifetime.

In this chapter, the polarity correlation method is applied to an experiment to measure the prompt neutron decay constant or the subcriticality in a graphite moderated and reflected reactor SHE-T-1 with the reactivity ranging widely from critical to almost shut down state (-12 dollars) without external disturbance such as pulsed neutron source.

5.2 Principle

When a reactor is operating at steady power, the count rate of neutron detector will fluctuate in time around its own mean count rate. The count rate is converted to polarity signal, or in other words, Sgn function signal, which has a logical + 1 value when the count rate exceeds the mean rate and has a logical -1 value when otherwise.

A polarity correlation function is defined as a correlation function of this polarity signal.

$$\phi_p(\tau) = \lim_{T\to\infty} \frac{1}{2T} \int_{-T}^{T} sgn\, \chi_1(t) \cdot sgn\, \chi_2(t+\tau)\, dt . \qquad (31)$$

When the statistical property of count rate χ is approximated to obey a two demensional Gaussian distribution, Eq. (31) is expressed as,

$$\phi_p(\tau) = \frac{2}{\pi} \sin^{-1} \phi(\tau) \ , \tag{32}$$

where $\phi(\tau)$ is a correlation function of χ. When the reactor kinetics is approximated by one-point model, the correlation function is expressed by a single exponential time function,

$$\phi(\tau) = A\, e^{-\alpha|\tau|} \ . \tag{33}$$

Furthermore, when the correlation amplitude A is enough smaller than 1, Eq. (32) becomes,

$$\phi_p(\tau) = \frac{2A}{\pi} e^{-\alpha|\tau|} \ . \tag{34}$$

Eq. (34) is used to analyze the experimental data.

A modified type of polarity correlation function is introduced by one of the authors[17], which is called a conditional polarity correlation function. When a neutron count rate reaches a preset level, conditioning pulse is generated. A conditional polarity correlation function is defined as a correlation function between the conditioning pulse and polarity signal (sgn function),

$$B(\mathrm{sgn}\, \chi_2 = +1 \,|\, \chi_1') = \frac{1}{2} + \frac{1}{\sqrt{2\pi}} \left(\frac{\chi_1'}{\sigma_1}\right) \phi(\tau) - O(\phi^3(\tau)) \ , \tag{35}$$

where: $B(\mathrm{sgn}\, \chi_2 = +1 \,|\, \chi_1')$ is defined as a type of conditional polarity correlation function which indicates that χ_2 has a positive polarity under the condition that χ_1 has a preset level χ_1'; σ_1 is the standard deviation of χ_1; O is a function

involving the higher order term, $(\phi(\tau))^n$; $\phi(\tau)$ is a correlation function between χ_1 and χ_2.

5.3 Experiments

Experiments are performed in SHE facility operating at very low power steady state with (subcritical) and without (critical) start up neutron source.

In SHE-T-1 core, the polarity correlation method is applied to the experiment for measuring the safety rod reactivity worth. The pulsed neutron and rod drop experiments are also performed for the purpose of comparison.

A large volume BF_3 proportional counter (84EB 45/50G, O.D. = 5 cm, L = 100 cm) is placed on the axis of cylindrical core to get a sufficient detection efficiency, in spite of inducing a strong depression to neutron flux distribution (reactivity worth is about 2.5 dollars). The SHE-T-1 core is loaded with 152 fuel rods to get critical. The polarity correlation method is applied to the experiment in this delayed critical core to obtain a prompt neutron decay constant at delayed critical.

The critical core is then made subcritical by inserting the safety rods. The number of safety rods inserted is varied from one to six. At each step of insertion, the polarity correlation, pulsed neutron and rod drop experiments are carried out to measure the subcriticality, i.e., reactivity worth of safety rods inserted.

In the polarity correlation experiments,[18] the neutron detection pulse is converted to clock-digitalized polarity

signal so as to get the delayed coincidence which is directly identical to the polarity correlation function. In Fig. 12, are drawn the decay curves of polarity correlation function against delay time for the various number of safety rods inserted.

The pulsed neutron experiments are done with the conditions almost as same as those described in chapter 3.

In the rod drop experiments, integration type analysis is chosen. The effects of the count start and stop time on integrated value are carefully examined to get a exact reactivity worth.

The reactivity worth is calculated from the prompt neutron decay constant using the original King-Simmon's formula Eq. (12), in both cases of polarity correlation and pulsed neutron experiments, while in case of rod drop experiment, the reactivity worth is calculated using the well-known formula for ^{235}U loaded core:

$$\rho/\beta_{eff} = (\text{count rate before rod drop/integrated counts after rod drop}) \times 13.01 \qquad (36)$$

The resultant values of reactivity worth are plotted against the number of safety rods inserted into the critical core and shown in Fig. 13. The reactivity worths, obtained by the three experimental methods at each number of safety rods inserted, show satisfactory agreements by about 4 ~ 7 % discrepancies.

In SHE-VIII core, the conditional polarity correlation experiment is performed for the purpose of demonstrating how

the theoretical expression can be observed in the experimental results. The experimental set up is similar to that of polarity correlation experiment, but in the former case, the critical core is unloaded with one fuel rod and a start up neutron source is introduced to it to make it a subcritical steady state, and two relatively small BF_3 proportional counters (Hitachi EB125 B-2, O.D. = 2.5 cm L = 30 cm) are utilized by setting at the boundary between core and reflector in mid plane. One detector signal is made to produce the conditioning preset signal, and starts a multi-channel time analyzer sweep, while the another detector signal is converted to polarity signal and its digitized positive part is fed to the analysis signal input of the analyzer.

A piece of conditional polarity correlation function measured is shown in Fig. 14 against delay time between x_1' and $sgn\ x_2 = +1$ for various values of conditioning preset level x_1'. After the investigation of such experimental data, three remarkable facts are pointed out: 1) The correlation amplitude is proportional to the conditioning preset level; 2) A common decay constant is possessed by all the decay curves for various conditioning preset level; 3) The decay constant is just the same as what is obtained by polarity correlation and pulsed neutron experiments. These facts support undoubtedly the theoretical expression in Eq. (35).

5.4 Discussions about the conditional polarity correlation

It has been proposed by several authors[19],[20],[21] that a chain enhanced part of neutron count rate can be

correlated with its following count rate, resulting to give a prompt neutron decay curve. Such a technique is called "Endogeneous pulsed source", or "Flash start technique". The well-known Ross-α method can be understood to be included in such a category. Concerning to the pulse type flash start technique, the Rossi-α formula and its variations are well developed from a statistical point of view. However, the analog signal type flash start technique has been used empirically only. Under the assumption that the count rate fluctuation obeys a Gaussian distribution, the analog signal type flash start technique can be easily formulated as shown in Eq. (37)

$$\langle \chi_2' \rangle = m_2 + \frac{\sigma_2}{\sigma_1} (\chi_1' - m_1) \phi(\tau) \ , \tag{37}$$

where

$\langle \chi_2' \rangle$ is the ensemble average of χ_2 under the condition that χ_1 takes a preset level value χ_1',

m_i is mean value of count rate χ_i, $m_i = \langle \chi_i \rangle$,

σ_i is the standard deviation of χ_i,

$\phi(\tau)$ is the correlation coefficient in a two dimensional Gaussian distribution.

Obviously, Eq. (35) is equivalent to Eq. (37) when the correlation coefficient $\phi(\tau)$ is enough small and near to zero.

In short, the endogenous pulsed source or flash start technique is confirmed completely with the theoretical expression using both the one point model for reactor and a Gaussian model for count rate fluctuation.

5.5 Conclusive remarks on the polarity correlation method

The prompt neutron decay constants in a reactor with a long prompt neutron lifetime can be measured satisfactorily by the polarity correlation method not only at critical but also down to about twelve dollars subcritical.

The subcriticality obtained from the prompt neutron decay constant using the original King-Simmon's formula showed fairly good agreements between polarity correlation and pulsed neutron experiment involving 4% discrepancies and agreed also with that obtained from rod drop experiment involving 7% discrepancies at most.

A conditional polarity correlation function is introduced, and thereby, the endogenous pulsed source or flash start technique, especially in case of analog signal type, is confirmed completely with the theoretical expression using both the one point model for reactor as well as a Gaussian distribution model for count rate fluctuation.

6. Conclusion

The discussions given in the proceeding chapters are summarized as follows,

(1) It is safe to expect the exisistence of the discrete time eigen-value or the prompt neutron decay constant even in the highly subcritical cores.

(2) The precise value of the prompt neutron decay constant can be determined by use of the least squares fitting considering the accompanied slow decay of the delayed neutron modes. Such consideration is very important to exclude the systematic errors to be included in the prompt neutron decay constants.

(3) The King-Simmons formula is revised so as to get valid even for the cases that neutron generation time is much different from that at critical. The accuracies of the corection calculations are checked by comparing the resulted reactivity values with those obtained by the other methods.

(4) Integral versions of the pulsed neutron, source multiplication, and rod drop methods were experimentally demonstrated and then the discrepancies of the measured reactivities which have even been reported among those methods were reduced so much as to be not appreciable in most cases, even though the measured values showed strong dependence on the every detector positions.

(5) Applicable reactivity range of the polarity correlation method was enlarged down to about 12$ subcritical.

Therefore, it can be concluded that the experimental methods to measure large negative reactivity in the graphite-moderated and reflected relatively small reactor cores like SHE are established down to 34 $ subcritical.

Acknowledgement

The authors wish to thank Mr. M. Takeuchi (JAERI) and Mr. S. Ueda (Miyazaki University) for their valuable help in performing experiments. The authors wish particularly to express their indebtedness to Dr. Y. Gotoh for his supporting the present work.

Therefore, it can be concluded that the experimental methods to measure large negative reactivity in the graphite-moderated and reflected relatively small reactor cores like SHE are established down to 34 $ subcritical.

Acknowledgement

The authors wish to thank Mr. M. Takeuchi (JAERI) and Mr. S. Ueda (Miyazaki University) for their valuable help in performing experiments. The authors wish particularly to express their indebtedness to Dr. Y. Gotoh for his supporting the present work.

REFERENCES

(1) PUROHIT, S.N. : Nucl. Sci. Eng., 9, 157 167 (1961).

(2) GARELIS, E. : ibid., 15, 296 304 (1963).

(3) KANEKO, Y. : Nucl. Sci. Technol. 3, 212 215 (1966).

(4) FURUHASHI, A. : J. At. Energy Soc. Japan, 4 [10], 677 684 (1962).

(5) KUCHLE, M. "Exponential and Critical Experiment, Vol. 2," International Atomic Energy Agency, Vienna (1964).

(6) SASTRE, C. and WEINSTOCK, V. Nucl. Sci. Eng., 20, 359 (1964).

(7) KANEKO, Y. OHKUBO, S. and AKINO, F. : Nucl. Sci. Eng. 50, 173 (1973).

(8) OHKUBO, S. KANEKO Y. and AKINO, F.:"Computer Code ALPHA-D for Analysis of Experimental Data in Pulsed Neutron Technique," JAERI-M-4525, Japan Atomic Energy Research Institute (1971).

(9) INOUE, K. et al : JAERI-1032, (1962).

(10) SUMITA, K. et al. : J. Nucl. Sci. Technol., 4, 328 (1967).

(11) AKINO, F. et al. : JAERI-M-1795 (1964).

(12) KANEKO, Y. et al. : J. Nucl. Sci. Technol., 4 400 407 (1967).

(13) KANEKO, Y. et al. : JAERI-M-4971 (1971).

(14) KANEKO, Y. : J. Nucl. Sci. Technol., 12, 402 412 (1975).

(15) KOSALY, G. et al. : J. Nucl. Energy, 26, 17 26 (1971).

(16) FOWLER, T.B. et al. : ORNL-3199

(17) Yasuda, H. et al. : J. Nucl. Sci. Technol. 10, 753 761 (1973)

(18) Yasuda, H. et al. : ibid. 9, 544 550 (1972)

(19) Szechter, T. et al. : Nukleonik, 11, (5) 240 (1968)

(20) Chwaszczewski, S. et al. : Nucl. Sci. Eng., 25, (2) 201 (1966)

(21) Uhrig, R.E. : "Random Noise Techniques in Nuclear Reactor Systems", (1970), Ronald Press.

Table 1 The physical and nuclear properties of the different core configurations of SHE

Configuration	$C/^{235}U$	Number of loaded fuel rods at delayed critical	Critical mass in U (kg)	Inner reflector R (cm)	Core radius R (cm)	Core length H (cm)	α_c
SHE-5	5378	219	5.29	0	35.7	240	5.73±0.07
SHE-6	4328	196	5.95	0	33.8	240	5.86±0.15
SHE-7	3276	173	6.99	0	31.8	240	6.48±0.29
SHE-8	2226	147	8.69	0	29.3	240	7.01±0.35
SHE-9	5378	298	7.20	44.4	60.8	240	3.86±0.34
SHE-T1	6628 ($C/^{232}Th$ 2560)	97	5.73	0	41.2	240	6.02±0.06

Table 2

Prompt neutron decay constant determined with and without consideration for the slow decay of the delayed-neutron modes

Number of Fuel rods	Reactivity (cent)	Prompt-Neutron Decay Constant, α $(sec)^{-1}$	
		Constant Background Method	Present Method
214	-66.9	8.99±0.04	9.32±0.04
215	-51.75	8.22±0.05	8.54±0.06

Table 3

Experimental results for reactivity worths of experimental control rods in ring geometry in SHE-8 and SHE-T1

Core	Number of experimental control rods	Number of loaded fuel rods	Distance between core axis and experimental control rod (cm)	$\alpha - \alpha_o$ [1] (sec^{-1})	ρ_{KS} (dollars)	ε_1 (dollars)	ε_2 (dollars)	ρ_{RRS} (dollars)	S (Measured)	S (Calculated)	ρ (Calculated) (dollars)
SHE—8	1	138	0	64.38±0.89	9.18±0.47	5.706	0.07029	15.66			16.26
		138	6.5	63.91±0.89	9.12±0.47	5.447	0.07025	15.33			15.86
		138	19.5	58.91±0.84	8.40±0.44	3.820	0.06979	12.93			13.23
		140	32.5	50.15±0.76	7.15±0.37	1.953	0.06880	9.720			9.610
		140	58.5	17.33±0.46	2.58±0.15	0.2372	0.05891	3.075			2.504
		140	71.5	8.40±0.35	1.20±0.08	0.1321	0.04687	1.468			1.146
	2	136	6.5	100.90±1.25	14.39±0.74	14.29	0.07228	29.86	0.9739	0.9636	30.56
		136	19.5	108.93±1.33	15.56±0.80	13.80	0.07255	30.60	1.183	1.187	31.41
		140	32.5	105.49±1.29	15.05±0.77	6.386	0.07244	22.66	1.166	1.179	22.66
		140	58.5	38.63±0.64	5.51±0.29	0.2410	0.06690	6.238	1.014	1.038	5.202
		140	71.5	17.60±0.44	2.51±0.14	0.1324	0.05853	2.893	0.9854	1.016	2.329
	3	134	6.5	118.11±1.42	16.85±0.87	22.15	0.07281	40.35	0.8774	0.8718	41.47
		134	19.5	146.58±1.70	20.91±1.07	28.75	0.07343	51.32	1.323	1.307	51.00
		140	32.5	152.27±1.75	21.72±1.11	13.65	0.07352	37.09	1.272	1.298	37.42
		140	58.5	59.83±0.85	8.54±0.44	-0.01829	0.06988	9.237	1.001	1.053	7.910
		140	71.5	26.60±0.53	3.80±0.20	0.06283	0.06346	4.210	0.9560	1.021	3.511
	6	128	19.5	196.83±2.19	28.08±1.44	89.41	0.07409	119.7	1.543	1.519	120.6
		128	32.5	243.16±2.64	34.69±1.77	47.87	0.07446	85.27	1.462	1.471	84.82
		140	58.5	135.33±1.59	19.31±0.99	-2.387	0.07321	18.47	1.001	1.017	15.28
		140	71.5	59.18±0.85	8.44±0.44	-0.5905	0.06982	8.563	0.9722	0.9848	6.774
SHE—T1	1	94	0	69.92±0.38	11.61±0.13	5.074	0.08949	17.87			17.66
		94	11.26	66.13±0.45	10.98±0.13	4.384	0.08921	16.49			16.38
		94	22.52	54.67±0.26	9.080±0.10	2.893	0.08815	12.92			13.30
		94	33.78	43.07±0.13	7.154±0.077	1.529	0.08658	9.449			9.778
		96	45.03	28.51±0.09	4.736±0.051	0.6207	0.08310	5.890			6.371
		96	56.29	17.36±0.06	2.884±0.031	0.2255	0.07753	3.461			3.676
	2	92	11.26	109.27±0.78	18.15±0.23	13.82	0.09131	33.78	1.024	1.037	33.97
		92	22.52	109.50±0.46	18.19±0.20	11.67	0.09132	31.68	1.226	1.205	32.03
		92	33.78	96.18±0.76	15.97±0.21	5.698	0.09086	23.28	1.232	1.202	23.51
		96	45.03	67.80±0.23	11.26±0.12	1.536	0.08934	13.96	1.185	1.134	14.45
		96	56.29	42.43±0.14	7.047±0.076	0.2074	0.08647	8.010	1.157	1.072	7.880
	3	90	11.26	132.5±0.6	22.01±0.25	23.49	0.09190	47.68	0.9638	0.9792	48.12
		90	22.52	148.8±1.4	24.70±0.35	25.23	0.09221	52.37	1.351	1.319	52.60
		90	33.78	143.4±2.4	23.81±0.47	13.12	0.09212	39.28	1.386	1.344	39.44
		96	45.03	105.6±0.24	17.54±0.19	2.738	0.09120	22.04	1.249	1.214	23.21
		96	56.29	66.47±0.16	11.04±0.12	-0.1128	0.08924	12.07	1.162	1.108	12.22

(1) stands for the prompt neutron decay constant of the standed cores before the experimental control rods are inserted. α_o is 14.32±0.29 sec^{-1} and 7.58±0.03 sec^{-1} for SHE-8 and SHE-T1 respectively. It is to be noted that the value of $\alpha - \alpha_o$, listed here is conected to the cases of the standed cores being critical.

Table 4

Experimental results of negative reactivity for various core configurations made subcritical with multiple experimental control rods

Core Configuration	Measured values (1) ($)						Calculated values by two group theory ($)	
	Pulsed neutron (2)			Source multiplication	Rod drop	Substitution by fuel rods worths		
	ρ_{KS}	ρ_{RKS}	$\bar{\rho}_{SJ}$	$\bar{\rho}_{SM}$	$\bar{\rho}_{ROD}$		CRODER	EQ-3
0C	0.6492	0.861	0.8007 (0.7984)	——	——	0.8130±0.02	0.8618	——
1C	11.63	17.55	17.76 (17.74)	16.45 (17.89)	——	——	17.66	18.70
2C	18.75	33.97	35.7 (3)	33.51 (36.78)	——	——	33.97	35.99
3C	22.67	47.84	50.1 (3)	40.96 (56.96)	——	——	48.12	52.74
6S	13.97	——	(13.77)	(14.25)	(12.86)	——	——	——

(1) The reactivity values listed here are corrected to the reactivity change due to insertions of detectors (7.3 ¢ at z=31cm) as well as Am-Be neutron source (3.3¢ at core center). The reactivity values in blanket stand for ones with all of the weights being unity in case of 6S and stand for ones with the adjoint function being unity in case of the other core configurations.

(2) The value of α_c used is $6.02 \pm 0.06\ sec^{-1}$

(3) Not yet final value

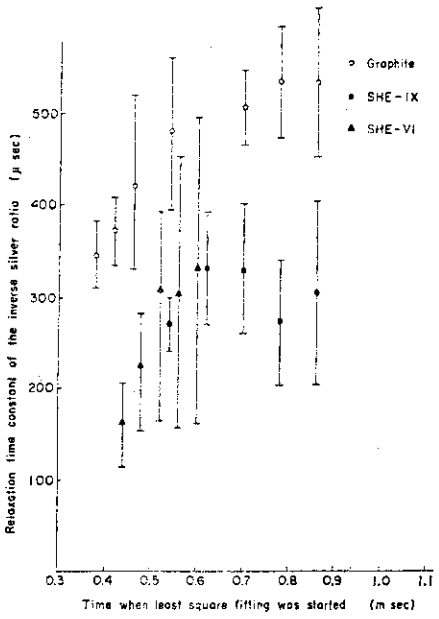

Fig. 1 Relaxation time constant of the inverse silver ratios in the graphite pile and the subcritical SHE-6 and -9

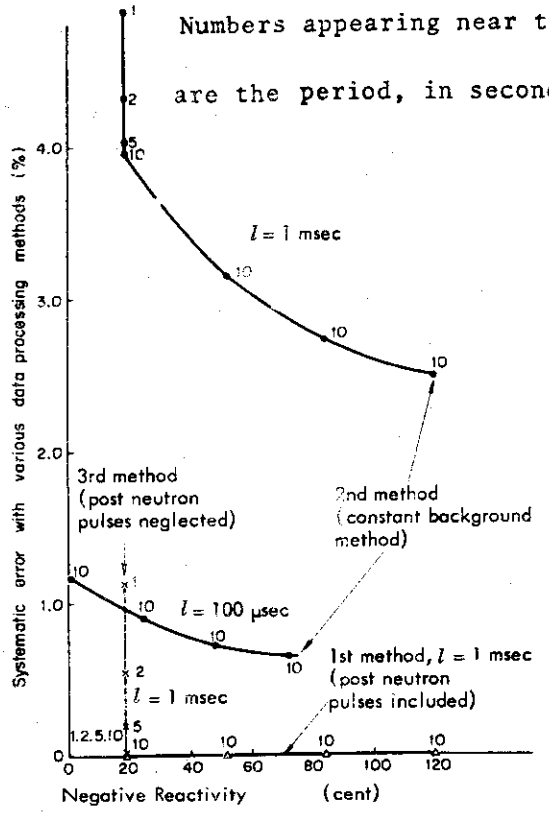

Fig. 2 Delayed-neutron effect on determination of prompt neutron decay constant, in a pulsed neutron experiment.

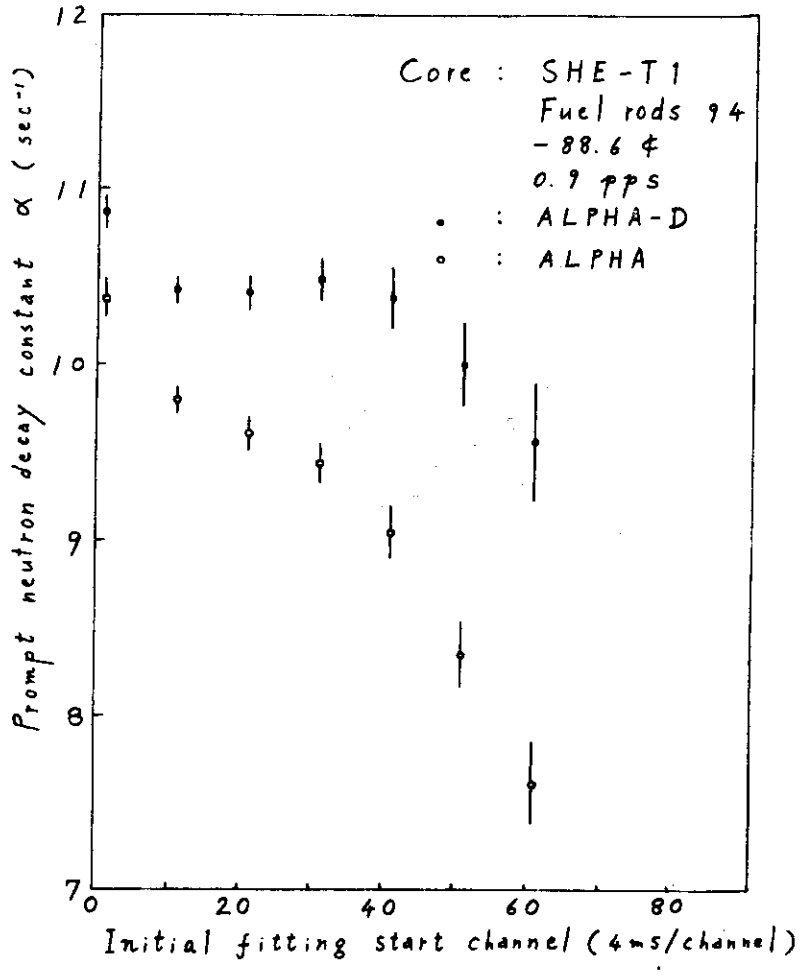

Fig. 3 Dependence of the value of α resulted by least squares fitting on the initial fitting start time from the pulsed neutron bursts.

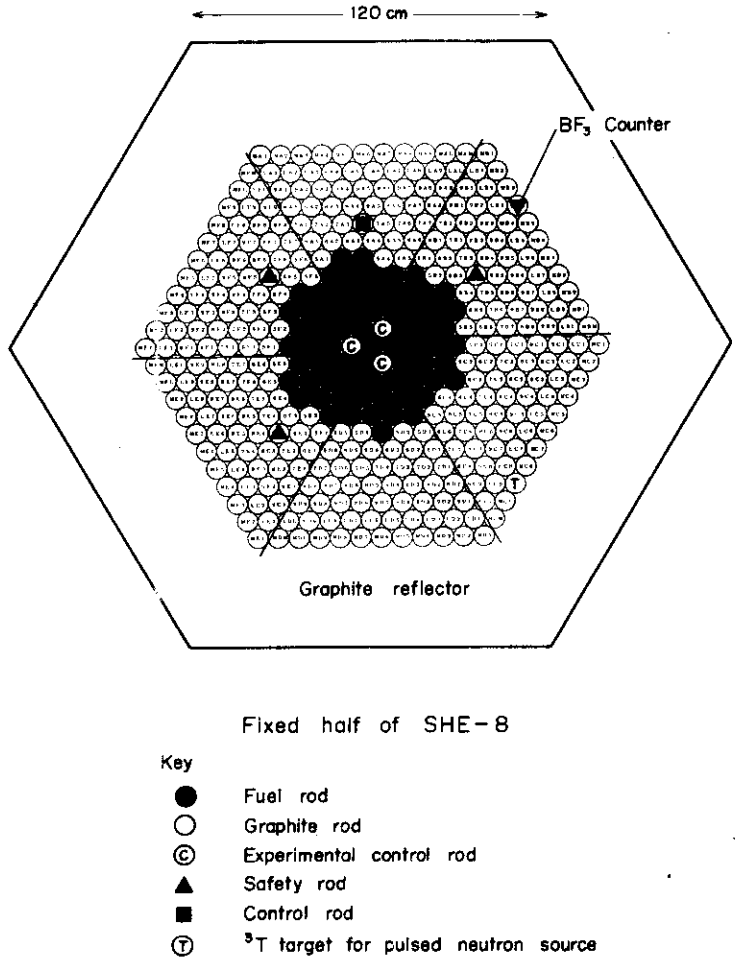

Fig. 4 Fuel loading patterns of SHE, and patterns of the experimental control rods configuration

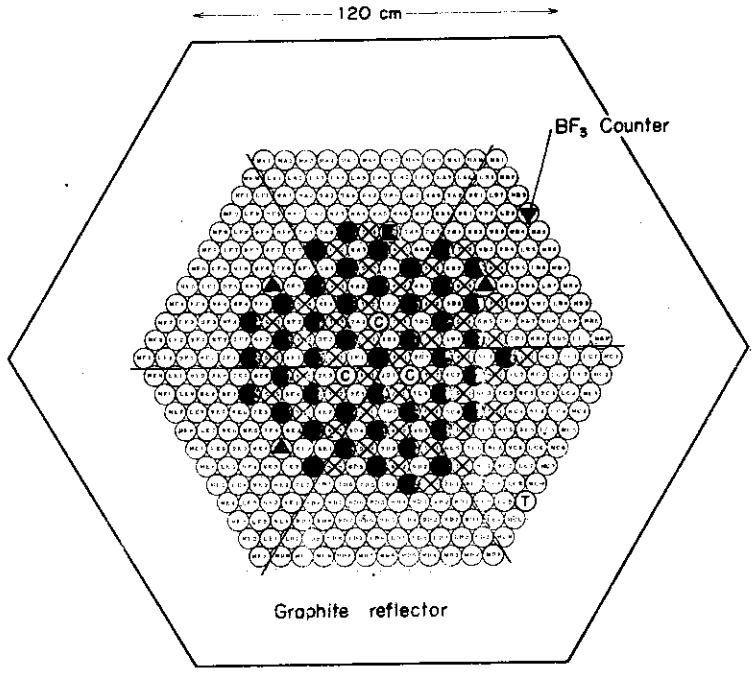

Fixed half of SHE-T1

Key

- ● Fuel rod
- ⊗ Thorium rod
- ○ Graphite rod
- Ⓒ Experimental control rod
- ▲ Safety rod
- ■ Control rod
- Ⓣ ^3T target for pulsed neutron source

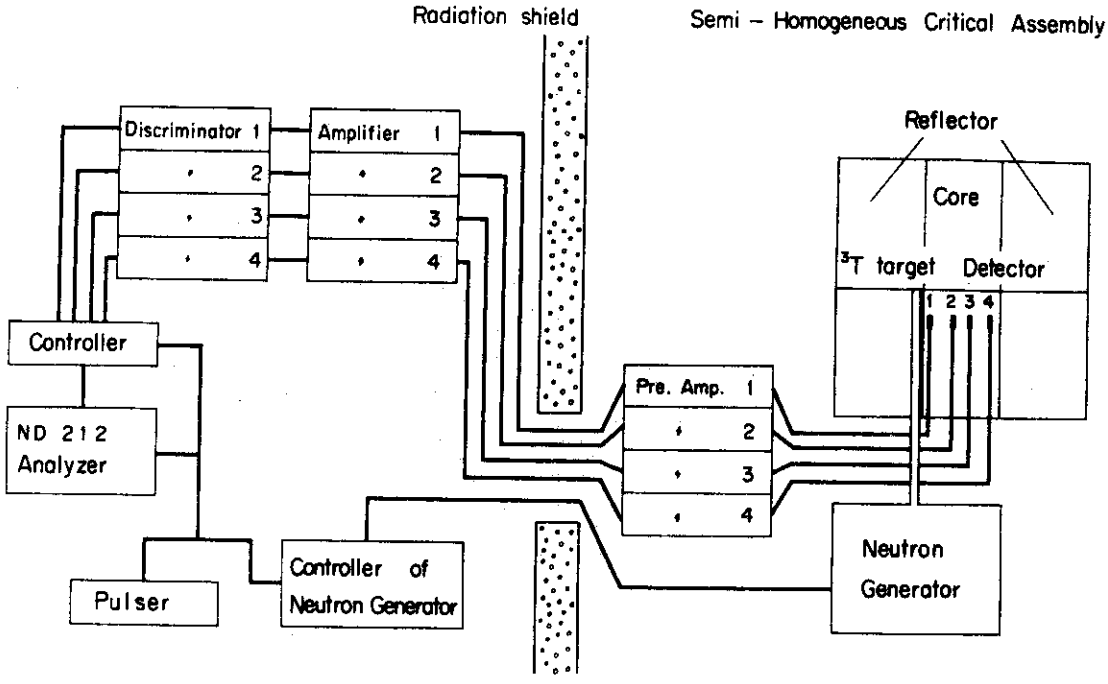

Fig. 5 Block diagram of the measuring system

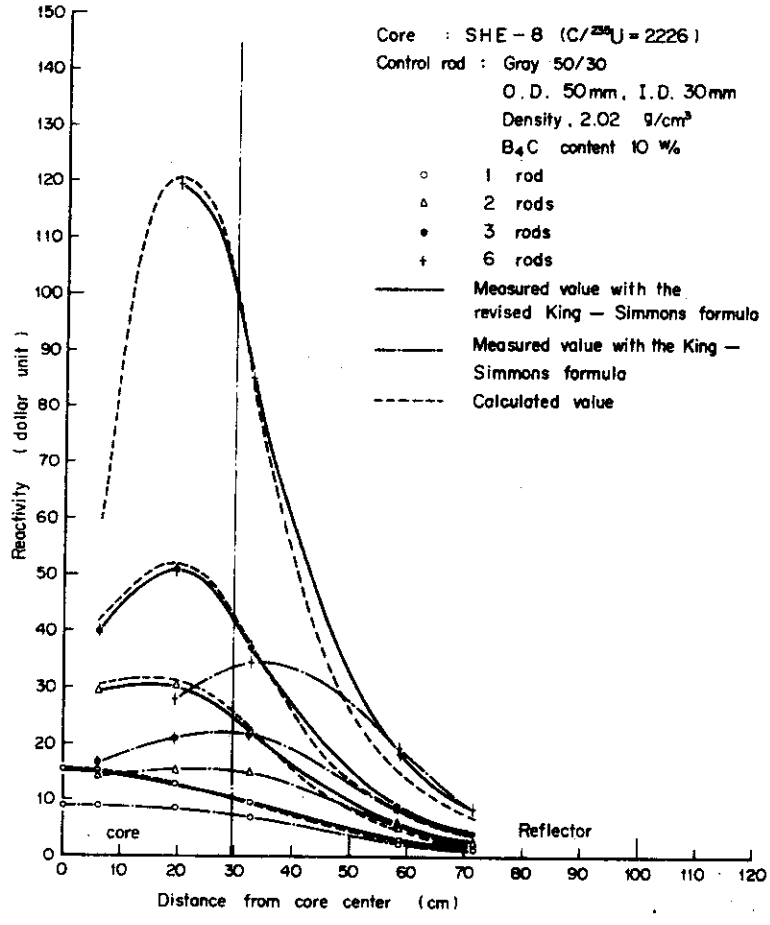

Fig. 6 Reactivity worths of the experimental control rods in ring geometries

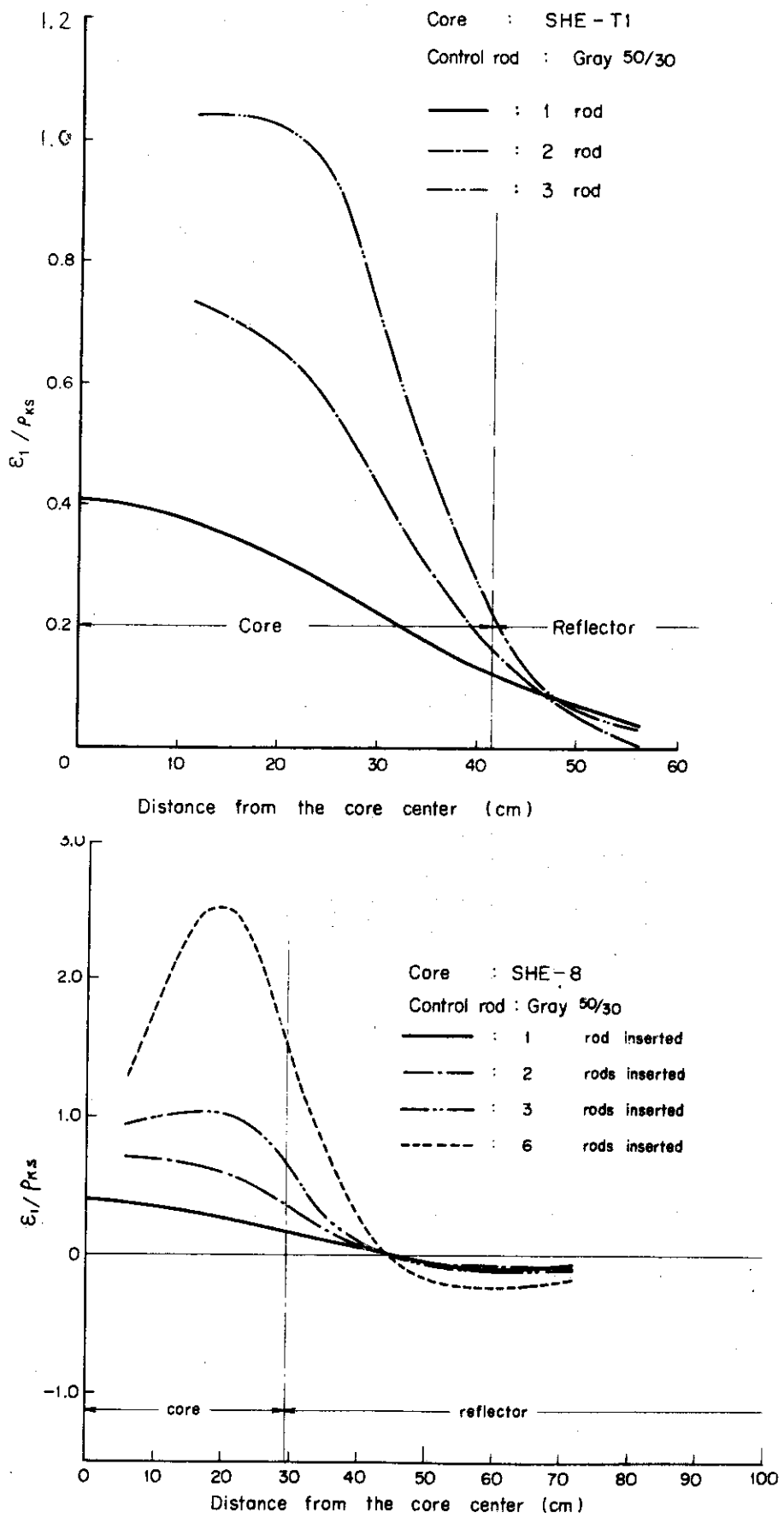

Fig. 7 Correction to the King-Simmons formula due to the change of the neutron generation time

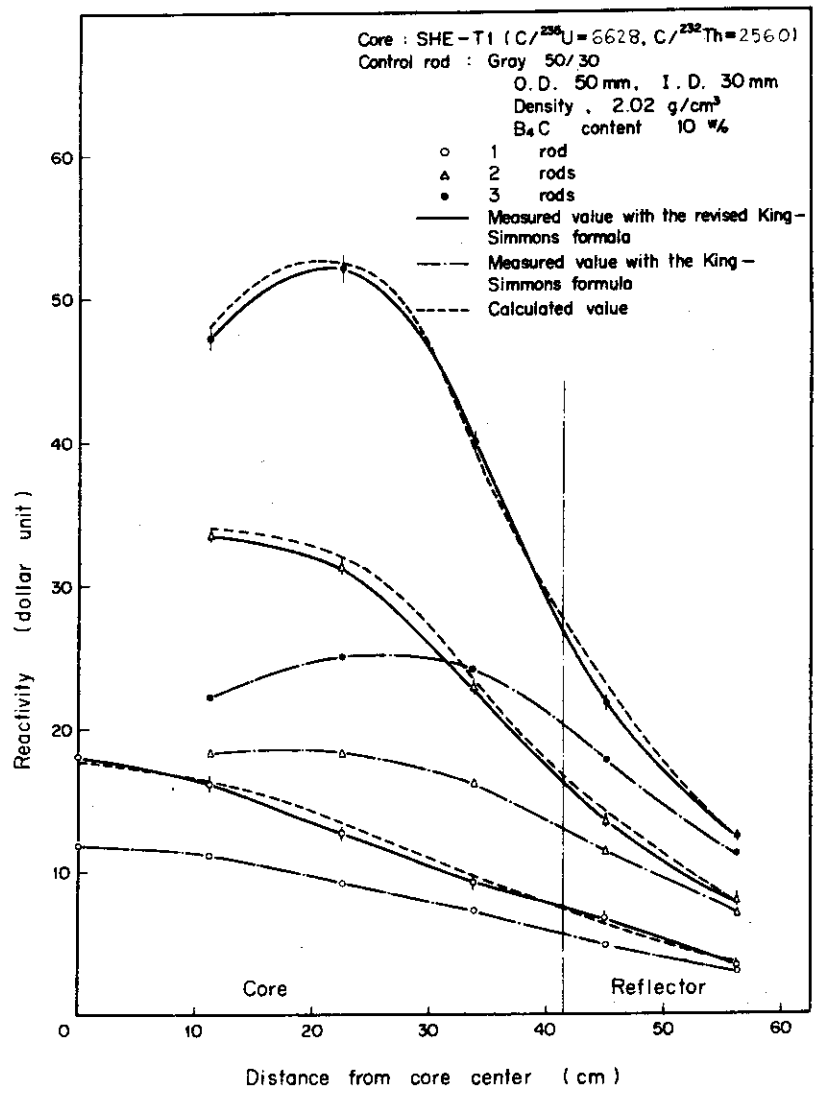
Core : SHE-T1 (C/^{235}U=6628, C/^{232}Th=2560)
Control rod : Gray 50/30
O.D. 50 mm, I.D. 30 mm
Density , 2.02 g/cm^3
B_4C content 10 w/o
1 rod
2 rods
3 rods
Measured value with the revised King-Simmons formula
Measured value with the King-Simmons formula
Calculated value
Reactivity (dollar unit)
Core
Reflector
Distance from core center (cm)
0
10
20
30
40
50
60

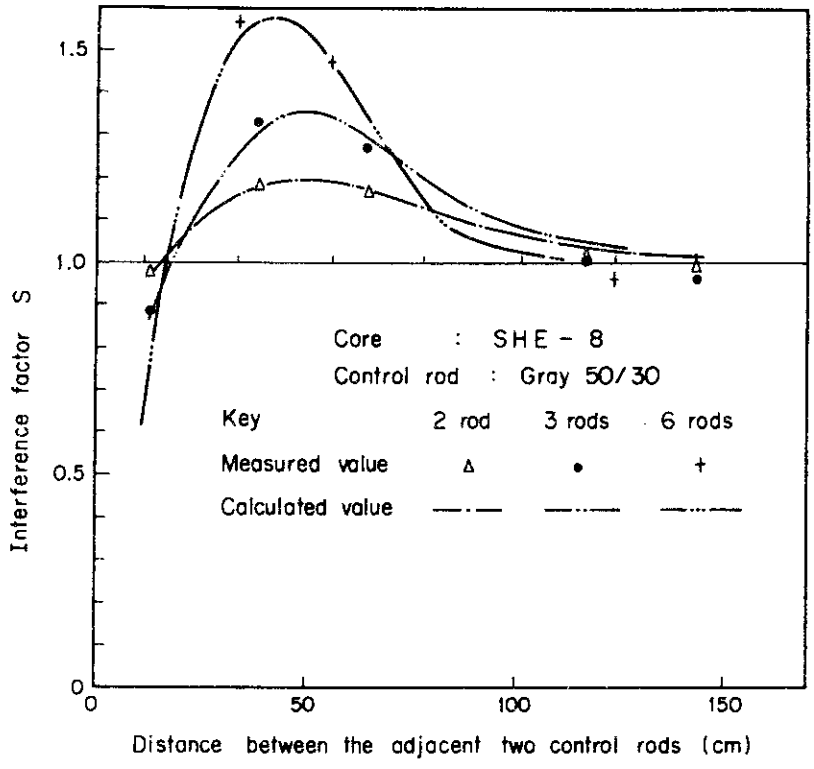

Fig. 8 Mutual interaction among experimental control rods arranged in ring geometry

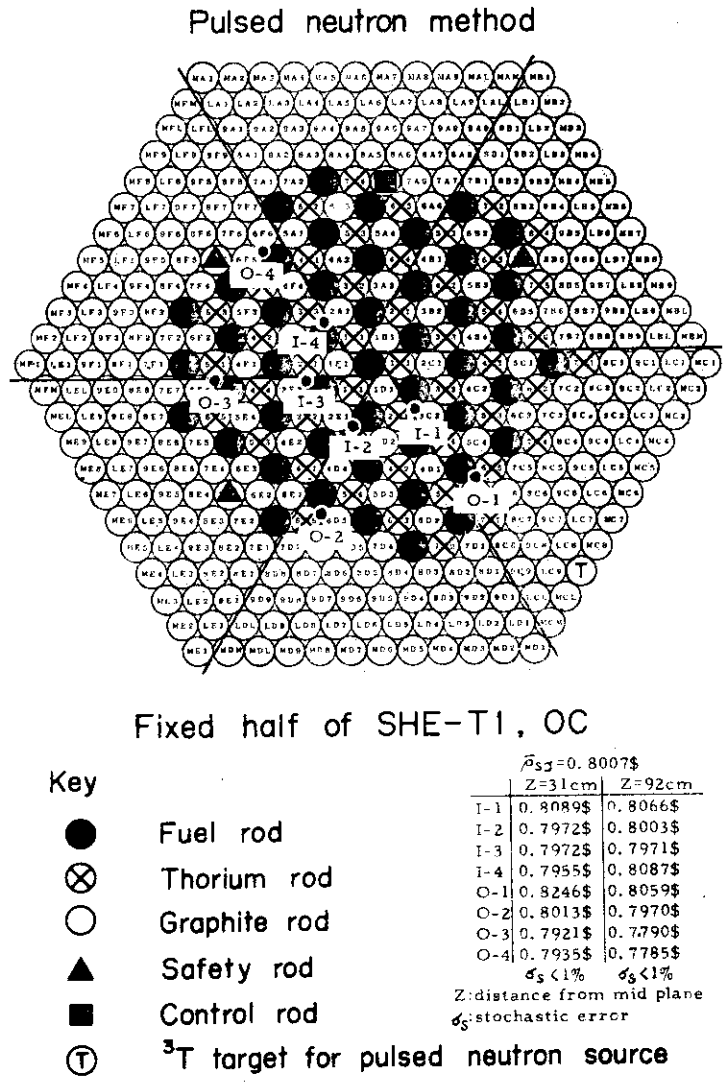

$\bar{\rho}_{S\mathfrak{J}}$=0.8007$

	Z=31cm	Z=92cm
I-1	0.8089$	0.8066$
I-2	0.7972$	0.8003$
I-3	0.7972$	0.7971$
I-4	0.7955$	0.8087$
O-1	0.8246$	0.8059$
O-2	0.8013$	0.7970$
O-3	0.7921$	0.7790$
O-4	0.7935$	0.7785$
	σ_S<1%	σ_S<1%

Z: distance from mid plane
σ_S: stochastic error

Fig. 9 Space-dependence of the reactivity values, obtained by single-point type formulas.

Pulsed neutron method

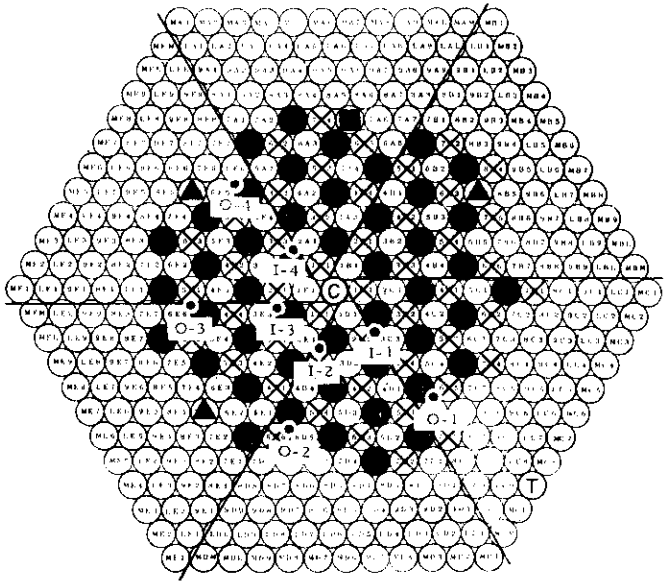

Fixed half of SHE-T1, 1C

Key

- ● Fuel rod
- ⊗ Thorium rod
- ○ Graphite rod
- Ⓒ Experimental control rod
- ▲ Safety rod
- ■ Control rod
- Ⓣ ^{3}T target for pulsed neutron source

I, O, : Detector position indices in core cross section

$\bar{\delta}_{SS}$=17.76$

	Z=31cm	Z=92cm
I-1	19.46$	18.14$
I-2	17.58$	19.04$
I-3	16.97$	16.76$
I-4	15.13$	16.59$
O-1	25.02$	20.69$
O-2	19.71$	18.89$
O-3	15.52$	15.34$
O-4	14.83$	13.37$
	σ_δ<2%	σ_δ<3%

Z:distance from mid plane
σ_δ:stochastic error

Pulsed neutron method

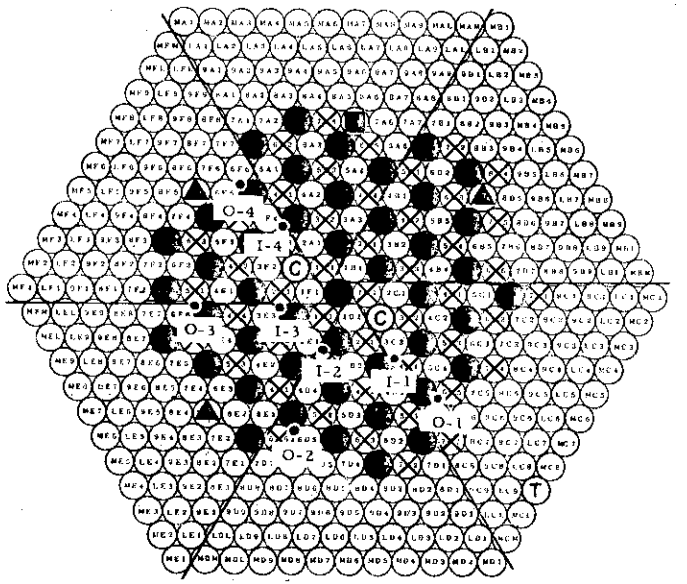

Fixed half of SHE-T1, 2C

Key

- ● Fuel rod
- ⊗ Thorium rod
- ○ Graphite rod
- Ⓒ Experimental control rod
- ▲ Safety rod
- ■ Control rod
- Ⓣ ^{3}T target for pulsed neutron source

I, O, : Detector position indices in core cross section

$\bar{\delta}_{SS}$=35.7$

	Z=31cm	Z=92cm
I-1	44.0$	31.2$
I-2	33.7$	30.9$
I-3	27.5$	28.2$
I-4	26.1$	25.3$
O-1	59.1$	42.0$
O-2	40.0$	32.0$
O-3	27.2$	23.5$
O-4	24.5$	23.9$
	σ_δ<3%	σ_δ<3%

These values are not yet final ones.
Z:distance from mid plane
σ_δ:stochastic error

Pulsed neutron method

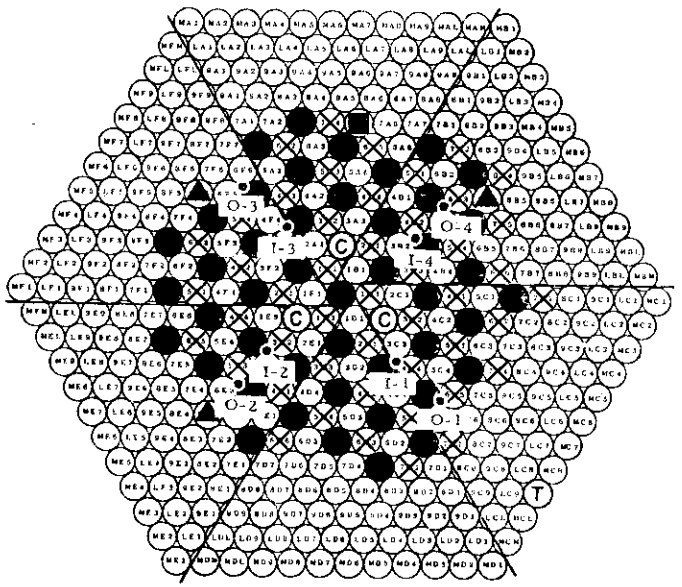

Fixed half of SHE-T1, 3C

Key

- ● Fuel rod
- ⊗ Thorium rod
- ○ Graphite rod
- Ⓒ Experimental control rod
- ▲ Safety rod
- ■ Control rod
- Ⓣ ^{3}T target for pulsed neutron source

$\bar{\gamma}_{SJ}$=50.1$

	Z=31cm	Z=92cm
I-1	81.6$	46.8$
I-2	49.8$	34.8$
I-3	35.4$	34.5$
I-4	41.1$	34.5$
O-1	90.8$	51.2$
O-2	43.7$	38.0$
O-3	32.9$	33.1$
O-4	49.2$	36.6$
	σ_S<3%	σ_S<3%

These values are not yet final ones.
Z: distance from mid plane
σ_S: stochastic error

I, O, : Detector position indices in core cross section

Pulsed neutron method

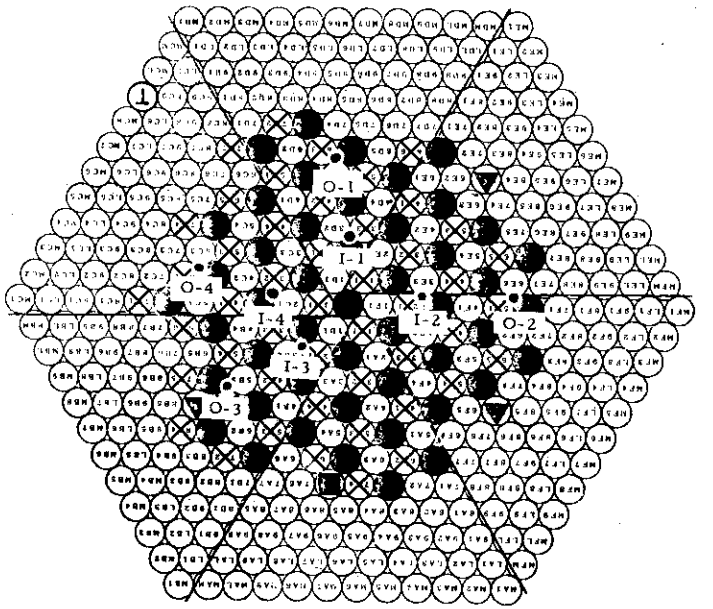

Fixed half of SHE-T1, 6S

Key

- ● Fuel rod
- ⊗ Thorium rod
- ○ Graphite rod
- ▲ Safety rod
- ■ Control rod
- Ⓣ ^{3}T target for pulsed neutron source

$\bar{\gamma}_{SJ}$ = (13.77 $)

	Z=31cm	Z=92cm
I-1	13.04$	12.48$
I-2	11.82$	12.81$
I-3	12.43$	12.85$
I-4	13.20$	13.35$
O-1	17.35$	15.55$
O-2	12.78$	10.32$
O-3	13.59$	11.27$
O-4	18.32$	13.76$
	σ_S<1.5%	σ_S<2%

Z: distance from mid plane
σ_S: stochastic error

I, O, : Detector position indices in core cross section

Rod drop method

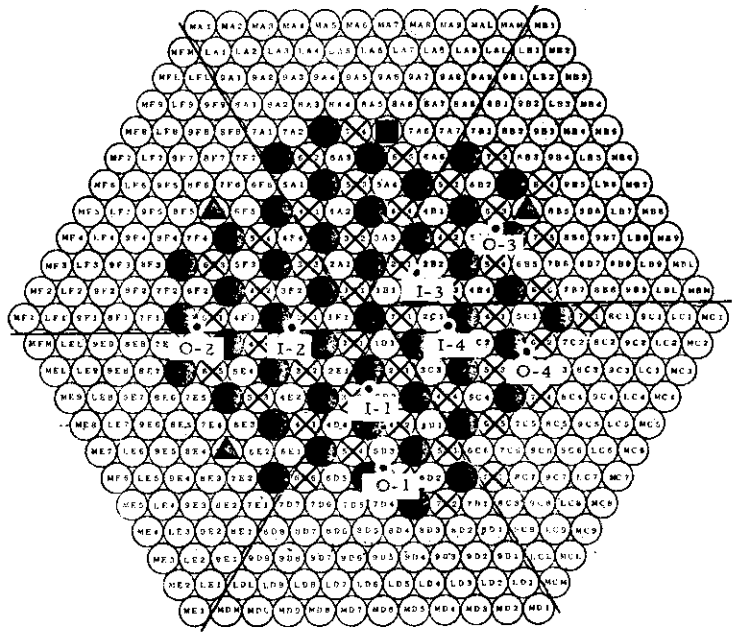

Fixed half of SHE-T1, 6S

Key

- Fuel rod
- Thorium rod
- Graphite rod
- Safety rod
- Control rod

$\bar{\rho}_{Rod}$ = 12.86$

	Z=31cm	Z=92cm
I-1	11.52$	13.01$
I-2	11.86$	13.62$
I-3	11.58$	12.99$
I-4	11.28$	12.82$
O-1	12.30$	12.80$
O-2	13.14$	15.18$
O-3	16.08$	19.45$
O-4	11.52$	12.84$
	σ_S<2%	σ_S<3%

Z: distance from mid plane

σ_S: stochastic error

I, O, . Detector position indices in core cross section

Source multiplication method

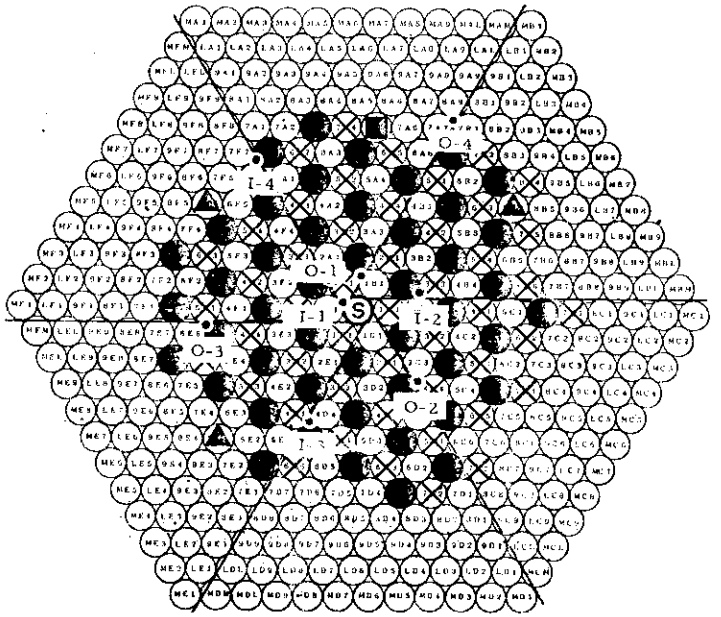

Fixed half of SHE-T I , OC

Key

- ● Fuel rod
- ⊗ Thorium rod
- ○ Graphite rod
- ▲ Safety rod
- ■ Control rod
- Ⓢ Neutron source

I, O, : Detector position indices in core cross section

Source multiplication method

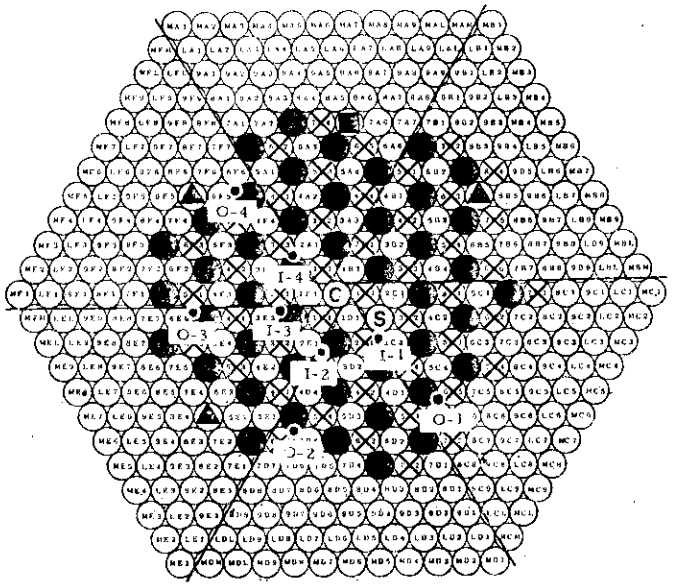

Fixed half of SHE-T1 , I C

Key

- ● Fuel rod
- ⊗ Thorium rod
- ○ Graphite rod
- Ⓒ Experimental control rod
- ▲ Safety rod
- ■ Control rod
- Ⓢ Neutron source

I, O, : Detector position indices in core cross section

Source multiplication method

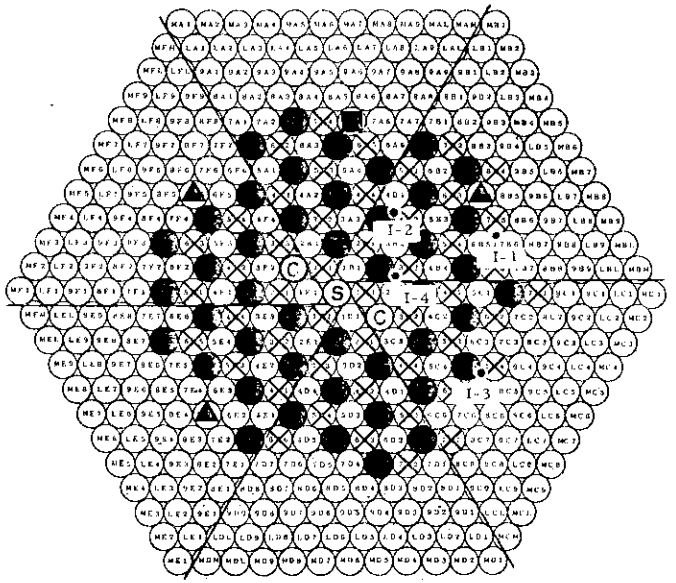

Fixed half of SHE-T1, 2C

Key

- Fuel rod
- Thorium rod
- Graphite rod
- Experimental control rod
- Safety rod
- Control rod
- Neutron source

I, O, : Detector position indices in core cross section

Source multiplication method

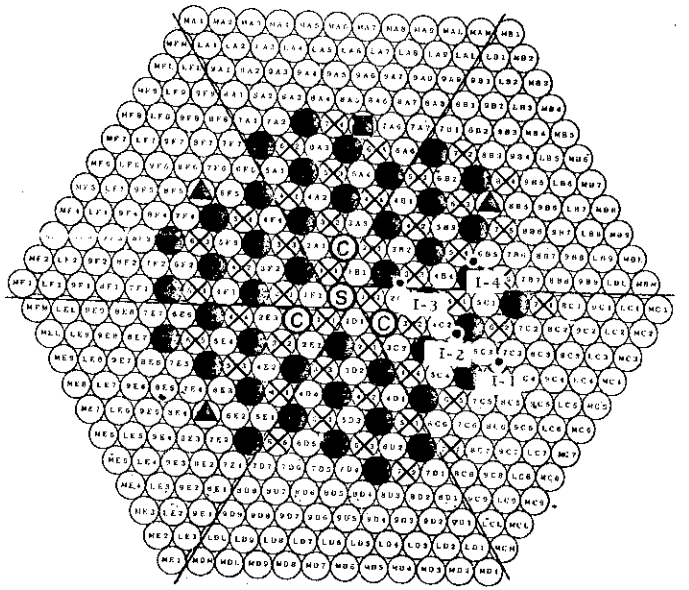

Fixed half of SHE-T1, 3C

Key

- Fuel rod
- Thorium rod
- Graphite rod
- Experimental control rod
- Safety rod
- Control rod
- Neutron source

I, O, : Detector position indices in core cross section

Source multiplication method

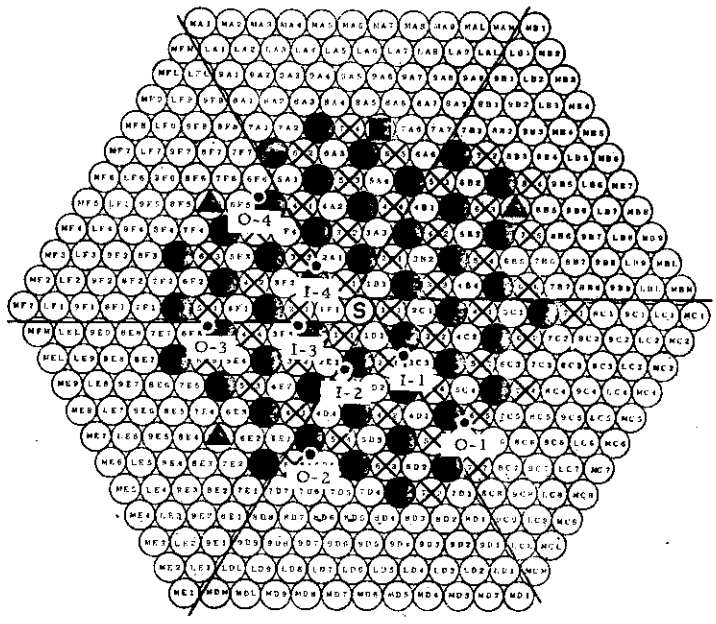

Fixed half of SHE, T-1, 6S

Key

- ● Fuel rod
- ⊗ Thorium rod
- ○ Graphite rod
- ▲ Safety rod
- ■ Control rod
- Ⓢ Neutron source

I, O, : Detector position indices in core cross section

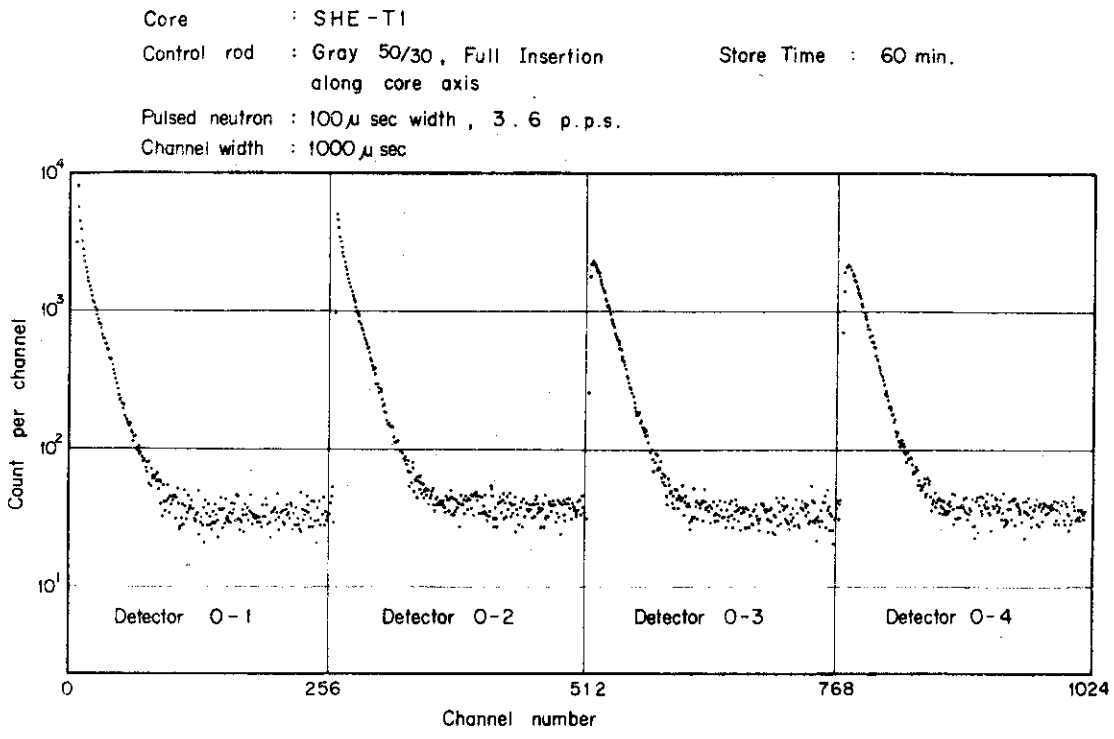

Fig. 10 Decay of neutron density following pulsed neutrons, stored in 1024 channel time analyzer, 254 channels for each of four neutron counting channels.

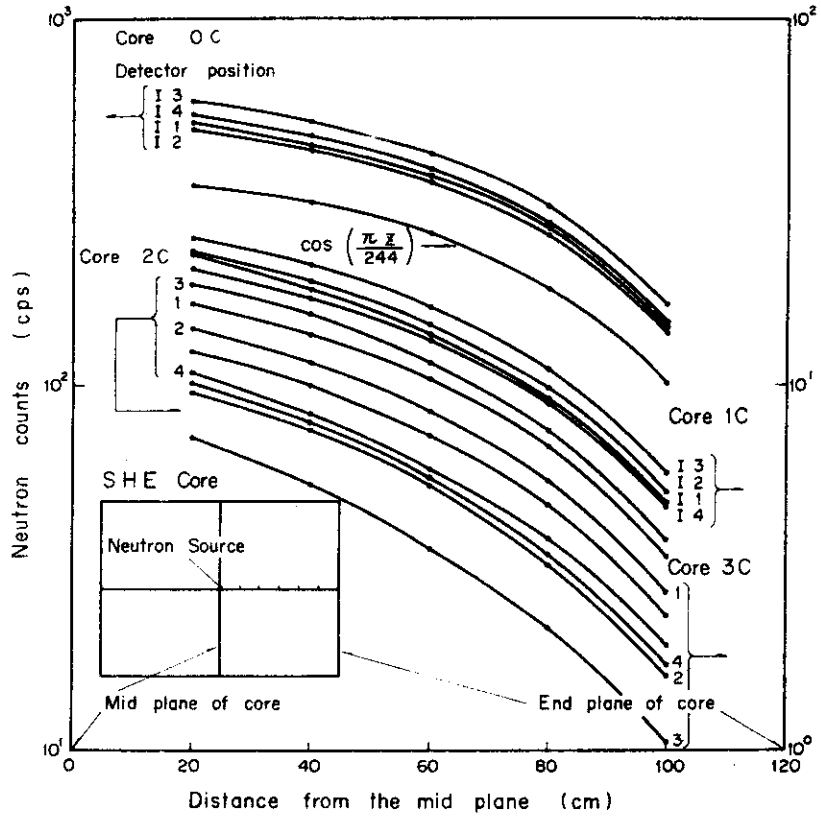

Fig. 11 Spatial distribution of the neutron counts in the core region of SHE-T1.

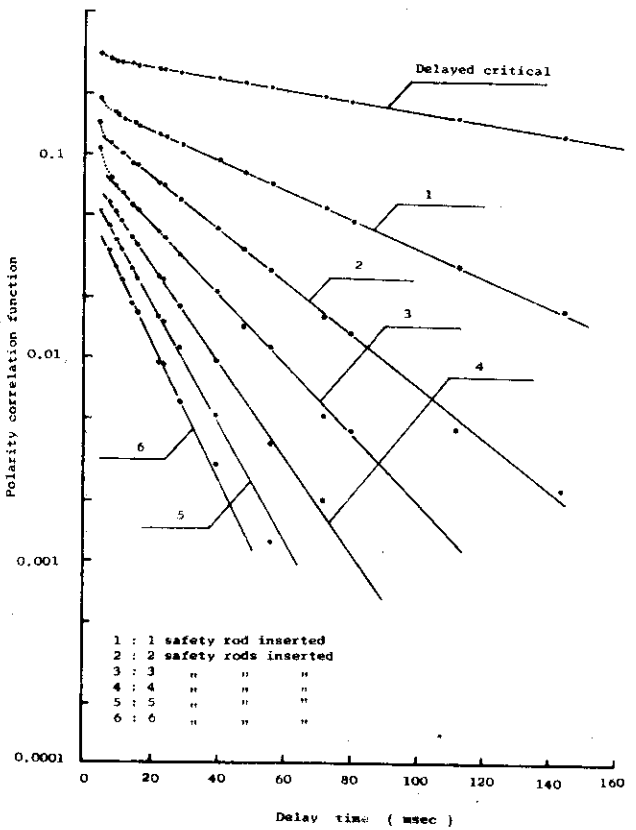

Fig. 12 Decay curves of polarity correlation function against delay time for the various number of safety rods inserted

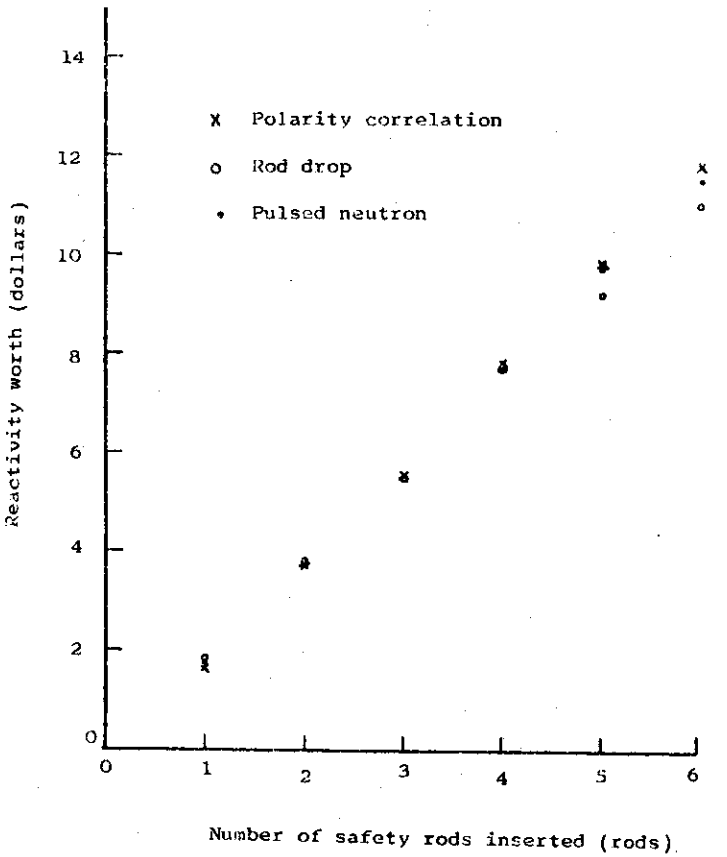

Fig. 13 Reactivity worths plotted against the number of safety rods inserted

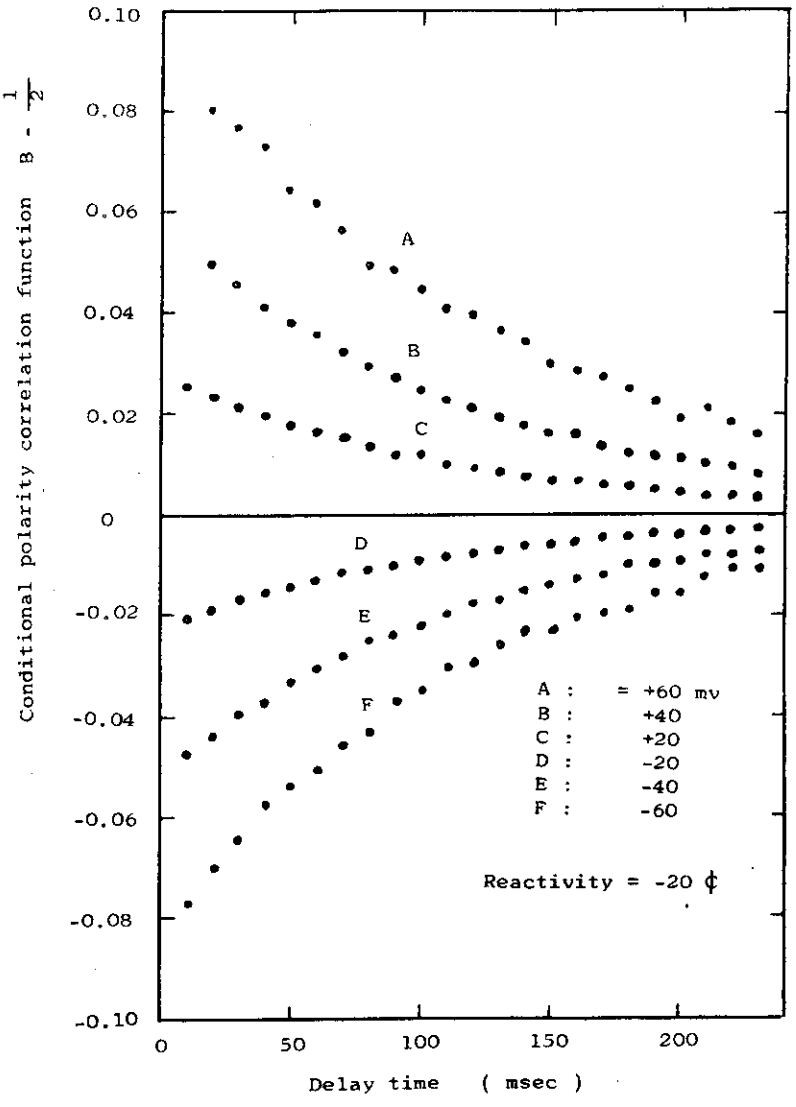

Fig. 14 Conditional polarity correlation function measured at -20¢ subcritical SHE-VIII-1 against delay time